

https://dspace.org/

The baseline assessment of radiological levels of water in the West Rand Region, Gauteng

Nkopo, Zandile Odessa

2022

https://hdl.handle.net/10539/37023

Downloaded from a DSpace repository. https://dspace.org/



WITS
UNIVERSITY

The baseline assessment of radiological levels of water in the West Rand Region, Gauteng

A Research Report submitted to the Faculty of Science, University of the Witwatersrand, Johannesburg, in partial fulfilment of the requirements for the degree of Master of Science in Hydrogeology

By

Zandile Odessa Nkopo

Student number: 682091

Supervisor: Prof. Tamiru Abiye

School of Geosciences, University of the Witwatersrand, P.O.Box Wits 2050, Braamfontein, Johannesburg

23 September 2022

Declaration

I declare that this research report is my own, unaided work. It is being submitted for the Degree of Master of Science in Hydrogeology at the University of the Witwatersrand, Johannesburg. It has not been submitted before any examination at any other University.

_____ _____

(Signature of candidate)

Day 23 of __ September 2022 __at ___The University of the Witwatersrand, Johannesburg___

Acknowledgements

I would like to express my sincere gratitude to my supervisor Professor Tamiru Abiye for your support, advice, and constructive criticism. Thank you for believing in me and allowing me to grow. Thank you.

To the National Nuclear Regulator's Centre for Nuclear Safety and Security (CNNS), I extend my most sincere gratitude. Thank you for awarding me this amazing opportunity and for the financial assistance, none of this would have been possible without you.

To Mr Mike Butler, thank you for your help with the ^{3}H and stable isotope analyses.

To Mr Madimetja Segobola, a warm thank you for all the support and assistance. You have truly been a great help and my go-to person whenever I needed help at the NNR.

To Seeke Carol Mohuba, I am very grateful for the support you showed me. Thank you for being patient with me and always pushing me to aim higher than the sky.

To Ms Monde Kakula, thank you for being the sister that you have been, for always listening to me and for always making time to listen to my problems. Your support is highly appreciated.

To my sister Nolithando Debra Nkopo, words fall short for the love and appreciation I have for you. You have been very supportive, and I will forever be in awe of that. Thank you for being my pillar of strength and an anchor that always kept me grounded and level-headed.

To Mr Mogomotsi Moeng, thank you for always encouraging me to keep going even when I had no energy left. You have truly kept me grounded through it all. Thank you.

To all my friends, family and everyone who contributed to this research, thank you for believing in me and thank you for the support.

Contents

..... i

Declaration ii

Acknowledgements iii

List of figures vi

List of tables vii

List of symbols viii

Nomenclature (abbreviations) ix

Abstract xi

Chapter 1: Introduction 1

1.1 Introduction 1

1.1.1 Problem statement 2

1.1.2 Aim and Objectives 2

1.2 Study Area 3

1.2.1 General overview 3

1.2.2 Geological and hydrogeological overview 5

Chapter 2: Literature review 9

2.1 The history of mining in South Africa 9

2.2 Acid mine drainage 9

2.2.1 The origin of AMD 9

2.2.2 The effects of AMD on water quality 10

2.3 Water quality 10

2.4 Radioactivity 12

2.4.2 The chemistry of elements 15

2.4.3 The mobility of radionuclides 19

2.5 Acceptable radiological levels in drinking water 20

2.6 Radioactivity in drinking water 21

2.6.1 South Africa 21

2.6.2 Other parts of the world 24

2.7 Health implications associated with radiation exposure 25

Chapter 3: Materials and Methods 26

3.1 Sampling 26

3.1.1 Site selection 26

3.1.2 Sampling 26

3.2 Sample analysis 29

3.2.1 Tritium analysis 29

3.2.2 Stable isotope analysis 30

3.2.3 Radionuclide analysis 30
Chapter 4: Results and Discussion 32
4.1 Physico-chemical parameters 32
4.2 Activity concentration and effective dose of radionuclides 33
4.2.1 Uranium 33
4.2.2 Thorium 39
4.2.3 Radium 47
4.2.4 Lead 49
4.2.5 Gross alpha 51
4.2.6 Gross beta 53
4.2.7 Effective dose 56
4.3 Stable isotopes within the study area 60
4.4 Tritium 64
4.5 A comparison of results from this study to previous studies 67
5. Conclusion 70
6. Recommendations 71
References 72

List of figures

Figure 1: A map illustrating the major towns within the West Rand region. 4
Figure 2: A geological map of the West Rand (Modified from the Council of Geosciences). 6
Figure 3: A hydrogeological representation of the West Rand region (Modified from the Department of Water and Sanitation). 8
Figure 4: An image illustrating the uranium and thorium decay series (source: World Nuclear Association, 2019). 14
Figure 5: An Eh-pH diagram showing the stability condition of (a) Th and (b) U (Kim and Osseo-Asare, 2012; Huang, 2016). 17
Figure 6: A map showing the locations of previous studies and threats associated with the findings of those studies. 23
Figure 7: Images showing sample collection (a) Vaal dam sample collection, (b) sample collection at a spring, (c) purging of pipes linked to borehole before sample collection and, (d) taking physico-chemical parameters in situ. 28
Figure 8: A map illustrating the distribution of ^{234}U within the West Rand. 34
Figure 9: A map illustrating the ^{235}U distribution within the West Rand. 36
Figure 10: A map showing the distribution of ^{238}U within the West Rand. 38
Figure 11: A map illustrating the ^{227} Th distribution within the West Rand. 40
Figure 12: A map illustrating the ^{228} Th distribution within the West Rand. 42
Figure 13: A map illustrating the ^{230} Th distribution within the West Rand. 44
Figure 14: A map illustrating the ^{232} Th distribution within the West Rand. 46
Figure 15: A map illustrating the ^{226}Ra distribution within the West Rand. 48
Figure 16: A map illustrating the ^{210}Pb distribution within the West Rand. 50
Figure 17: A spatial distribution map illustrating the gross-α activity distribution in the study area. 52
Figure 18: A spatial distribution map illustrating the gross beta activity distribution in the study area. 54
Figure 19: A comparative plot showing the measured radionuclide activity concentrations versus the recommended activity concentrations. 55
Figure 20: A graph showing the stable isotopes in groundwater versus the Johannesburg Local Meteoric Water Line (Leketa et al., 2019) and the Global Meteoric Waterline (Terzer et al., 2013). 61
Figure 21: The graph of d-excess against $\delta^{18}O$ for surface and groundwater samples in the West Rand. 63
Figure 22: A scatter plot showing the relationship between $\delta^{18}O$ and the residence time. 65
Figure 23: A spatial distribution map for ^{3}H for six groundwater samples. 66

List of tables

Table 1: Physico-chemical parameters for six groundwater samples within the study area. 33
Table 2: A table illustrating the effective dose (*e*) from ingestion of the radionuclides of interest in Sv/L..... 58
Table 3: A data table of the d-excess of groundwater samples in the study area..... 62
Table 4: Six water samples with their activity concentration, stable isotopes, and tritium data. 64
Table 5: Mean activity concentrations (mBq/L) for the radionuclides of interest from this study compared with the relevant drinking water guidelines and literature values. 67

List of symbols

‰ – Parts per mil

α – Alpha

A – Amperes

β - Beta

Bq/L – Becquerel per Litre

e – Effective Dose

^{2}H/D - Deuterium

^{3}H – Tritium

L/day – Litres per day

mg/L – milligrams per Litre

mL- millilitre

mSv/yr. – millisieverts per year

ppm – parts per million

TU – Tritium Units

Nomenclature (abbreviations)

AMD – Acid mine drainage

Ave. – Average

CA – Citric Acid

DWAF – Department of Water Affairs and Forestry

EC – Electrical Conductivity

EDTA – Ethylenediaminetetraacetic Acid

EPA – Environmental Protection Agency

FA – Fulvic Acid

GMWL- Global Meteoric Water Line

IDC – Individual Dose Criterion

JLMWL- Johannesburg Local Meteoric Water Line

LIWA – Liquid Water Isotope Analyzer

MDA – Minimum Detectable Activity

Min – Minimum

Max - Maximum

NECSA – South African Nuclear Energy Corporation

NORMs – Naturally Occurring Radioactive Materials

PTFE - Polytetrafluoroethylene

TDS - Total Dissolved Solids

WHO – World Health Organization

Abstract

Gold mining is one of South Africa's economic injectors. Given South Africa's unique geology, acid mine drainage (AMD) formed by mining activities allows for the dissolution and leaching of radionuclides into groundwater and potentially other drinking water sources under the right conditions. The aim of this study was to establish the baseline radiological levels of drinking water in the West Rand region of the Gauteng Province, South Africa. 23 water samples were collected from 9 towns within the study area and a liquid scintillation counter and Liquid Water Isotopes Analyzer (LIWA) model 45-EP were used for the analysis of tritium and stable isotopes respectively. Moreover, alpha spectrometry was employed for radionuclide analysis. Gross-α and gross-β activity concentrations were measured to determine the composition of radionuclides and identify the dominant radionuclides. The lowest activity concentration results reported were 15.3 mBq/L, 0.218 mBq/L, 4.73 mBq/L for uranium isotopes (^{234}U, ^{235}U, ^{238}U); 2.28 mBq/L, 4.73 mBq/L, 18 mBq/L, 2.71 mBq/L for thorium isotopes (^{227}Th, ^{228}Th, ^{230}Th, ^{232}Th); -9.8 mBq/L, -34 mBq/L, -6.4 mBq/L for radium isotopes (^{223}Ra, ^{224}Ra, ^{226}Ra); 1.2 mBq/L ^{210}Pb, -16 mBq/L and -1100 mBq/L gross-α and gross-β respectively.. The highest activity concentrations reported were 210 mBq/L, 2.85 mBq/L, 62.0 for uranium isotopes (^{234}U, ^{235}U, ^{238}U); 50.5 mBq/L, 33 mBq/L, 86.4 mBq/L and 23.5 mBq/L for thorium isotopes (^{227}Th, ^{228}Th, ^{230}Th, ^{232}Th); 13 mBq/L, 25 mBq/L and 19.5 mBq/L for radium isotopes (^{223}Ra, ^{224}Ra, ^{226}Ra); 135 mBq/L ^{210}Pb; 341 mBq/L and 13500 mBq/L for gross-α and gross-β respectively. The effective dose calculated from activity concentrations of all samples was within the allowed range (1 mSv/L to 3 mSv/L) of the WHO, UNSCEAR and DWAF drinking water guidelines. The low activity concentrations measured from the radionuclides suggest that the consumption of groundwater within the study area poses very little threat to human health but may cause severe health effects if it accumulates in the human body. The environmental isotopes results showed multiple moisture sources from global circulation, depleted $\delta^{18}O$ and $\delta^{2}H$ (-6.9‰ and -32.2‰, respectively) indicating that the recharging water underwent evaporation prior to recharge. Tritium was used to estimate the groundwater residence times and its activity concentration ranged from 9.44 to 28.32 mBq/L. Low ^{3}H activity concentrations are indicative of new to relatively young waters.

Keywords: Gold mining, radiological assessment, stable isotopes, tritium, water quality, radiation in drinking water.

Chapter 1: Introduction

1.1 Introduction

Water is an essential resource for all living organisms. In a time when the population is growing exponentially, the availability of fresh water and its quality is becoming a great concern (Durand, 2007). It is for this reason that water must always be used sparingly. Due to its neutral character, water can retain and carry most substances it comes into contact with. Water acts as a transporting mechanism for the dissolved radionuclides and other harmful minerals from one water source to the other and may percolate through the soil into the groundwater (Faanu *et al.*, 2011; WHO, 2011). Once the radionuclides are absorbed into the soil and water (including groundwater), there may be health implications such as exposure to radiation which may cause illness (Faanu *et al.*, 2011; WHO, 2011). Mining processes can be associated with the production of some radionuclides, which in the long term, have negative health impacts (Magagula, 2015). Other sources of radiation range from cosmic rays to the surface of the Earth. These sources of radiation directly affect the atmospheric concentrations of radionuclides (Faanu *et al.*, 2011; Magagula, 2015). The atmospheric radionuclide concentration must remain low to acceptable levels (Faanu *et al.*, 2011). However, the accumulation of radionuclides in soil, water and the atmosphere may increase due to industrial activities such as mining or engineering projects such as road construction (Faanu *et al.*, 2011), both of which involve excavating the Earth.

Radionuclides undergo radioactive decay through the emission of alpha particles, beta particles, or gamma rays. Naturally Occurring Radioactive Materials (NORMs) are abundant trace elements found in rocks, soil and water. Radionuclides that are associated with health risks are characterised by emitting alpha particles and beta particles. Drinking water could contain NORMs such as uranium, radium, and thorium (^{232}Th) decay series, their decay products, potassium (^{40}K) and artificial radionuclides (^{137}Cs, ^{134}Cs, ^{90}Sr, etc.). NORMs derived from ^{238}U, ^{235}U and ^{232}Th originate from the uranium, thorium, and actinium decay chain, respectively (Faanu *et al.*, 2011; Milenkovic *et al.*, 2019). Each decay chain follows a specific sequence, producing various isotopes that also emit either an alpha or a beta particle until a stable configuration is achieved (Skipperud and Salbu, 2018). Most of the products formed from the U decay chain are known to be radiotoxic (Boekhout *et al.*, 2015). Out of all the U decay chain products, radium is highly toxic and can induce cancers (Rachkova and

Shaposhnikova, 2020). The presence of radionuclides in water is dependent on the disintegration of the parent element. For example, ^{238}U (parent product of ^{226}Ra) has the lowest mobility in oxygen-poor groundwater and tends to be highly adsorbed by humic substances. However, the opposite is true for radium as it is highly mobile in anoxic groundwater with chloride and total dissolved solids (TDS) concentrations (Faanu *et al*., 2011; Milenkovic *et al*., 2019). Radium has similar chemical properties to other divalent alkaline-Earth cations such as calcium, strontium, and barium. Therefore, in aquifers with limited sorption or ion-exchange conditions, the common-ion effect enhances competition amongst the cations (Milenkovic *et al*., 2019). The main radium isotope in groundwater is ^{226}Ra, an alpha emitter with a half-life of 1622 years (Faanu *et al*., 2011; Milenkovic *et al.*, 2019).

1.1.1 Problem statement

Over the centuries, the mining industry has been a key player in the economy of South Africa. As important as mining is for the country, it has some negative effects on the environment and the surrounding communities. Gold occurs ubiquitously in the West Rand region. It is usually found in sulphide-rich ore bodies that contain a high concentration of Uranium and other daughter radionuclides as accessory minerals (Akcil and Koldas, 2006; Groudev *et al*., 2008; McCarthy, 2011). Due to the association of uranium-bearing minerals such as uraninite (UO_2) with gold, gold mining companies in the past were discarding slimes rich in uranium and later started extracting it. The resulting sulphide-rich large heaps of tailings are then exposed to atmospheric conditions and undergo oxidation forming acidic mine drainage (AMD) with elevated levels of heavy metals and radionuclides (Groudev *et al*., 2008; Madzivire *et al*., 2013). The AMD has the potential to mobilise and disperse the metals and radionuclides which may eventually join the groundwater system. Once the groundwater system is contaminated, the water in the neighbouring communities may be unsafe for consumption. Therefore, there is a possibility for the population to be exposed to radionuclides if untreated water is consumed and the exposure may have adverse health effects for those who consume it.

1.1.2 Aim and Objectives

The study aimed to establish the current status-quo of radionuclide levels in the water supply obtained from dams, springs, and taps in the West Rand region, Gauteng Province, South Africa. Due to widespread radionuclides in the different geological environments in South

Africa, it is necessary to determine and understand the background level of radionuclides in water that is destined for human consumption. This will ensure that chronic diseases related to radioactivity and metal ingestion are avoided.

The objectives of this study were to:

i. Determine the activity concentration and composition of radionuclides in the raw water (dams, springs, boreholes) and water that is distributed to the community.

ii. Determine the moisture source and relative age of water through radioactive and stable isotopes.

iii. Assess the water quality and the resulting health issues due to water consumption.

iv. Determine the effect of some chemical parameters on the mobility of radionuclides.

1.2 Study Area

1.2.1 General overview

The study was conducted in parts of the West Rand region, located in the Gauteng Province, roughly 30 km west of Johannesburg (Figure 1). The West Rand region covers an area from Randfontein in the west to Roodepoort in the east with coordinates 26.628889°S and 27.949008°E. It covers an area of 4 095 km^2 and falls within the highveld region of the Gauteng Province. This region was historically termed as a mining region due to the extensive gold mining which took place in the past century. It has since evolved and encompasses residential areas. Now, it also has agricultural and a few other land uses. Moreover, the region is characterised by decommissioned mines and abandoned tailings dams. The study area experiences a classic highveld climate with temperate summers with warm temperatures between November and February, while moderate to cool winter temperatures are experienced between June and August (Durand, 2007; Moshupya *et al.*, 2019). The West Rand region receives the highest rainfall during the summer months, usually between December and January (98mm). Very little to no rainfall is received during the winter months (as little as 20mm).

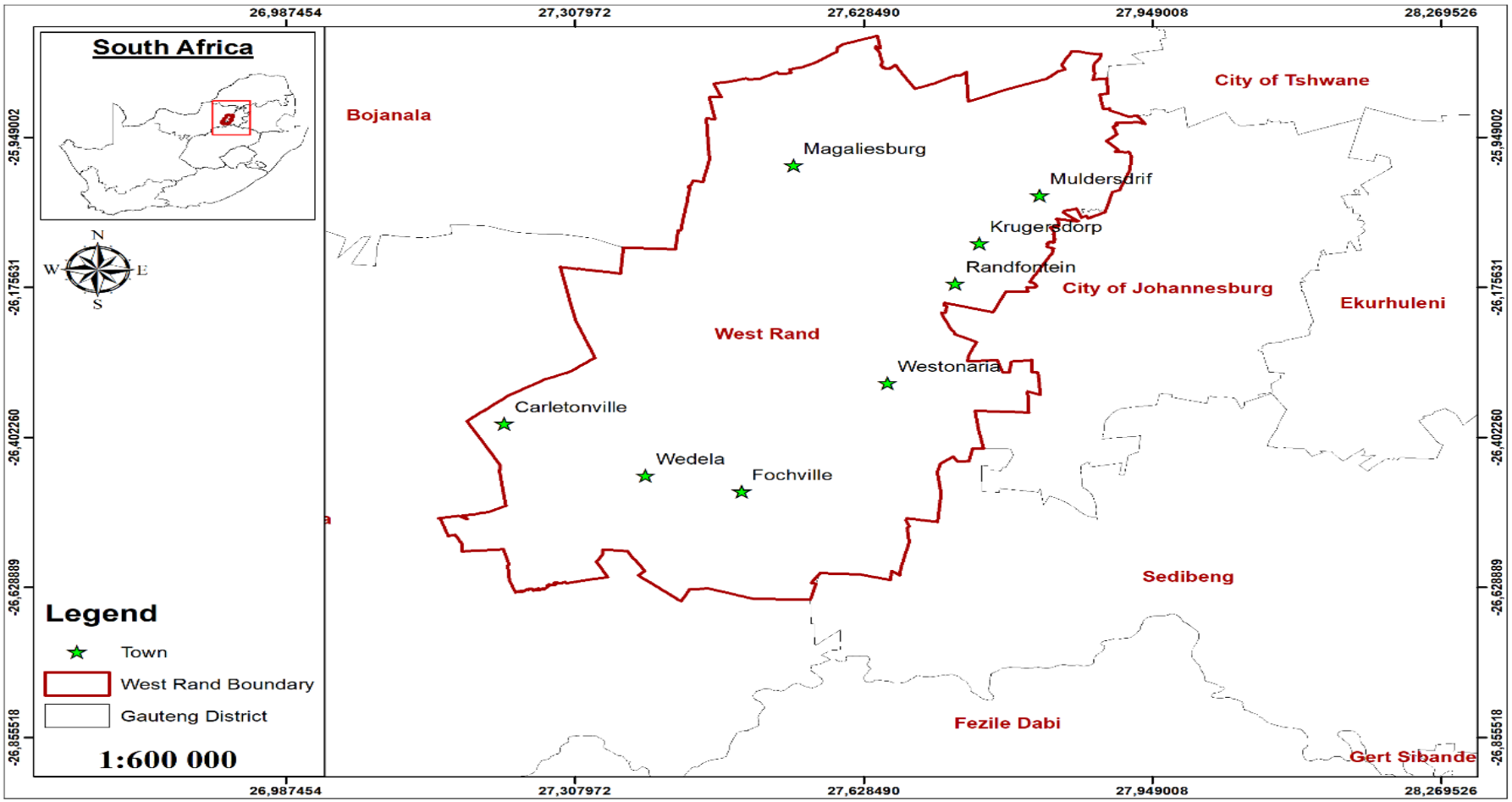

***Figure 1**: A map illustrating the major towns within the West Rand region.*

1.2.2 Geological and hydrogeological overview

The West Rand region has very distinct geology, which is characterised by the Witwatersrand Supergroup with the metasedimentary rocks of the West Rand and Central Rand Groups (Robb et al., 1997; Hobbs and Cobbing, 2007; Moshupya *et al.*, 2019). The West Rand Group is split into three subgroups: the Hospital Hill, Government Reef and the Jeppestown Subgroups (Durand, 2012). The Central Rand is also split into two subgroups: the Johannesburg and Turffontein Subgroups (Hobbs and Cobbing, 2007; Durand, 2012). The lithologies which dominate the study area include quartzites of the Government, Johannesburg, and Turffontein Subgroups (Hobbs and Cobbing, 2007). The area is also rich in well sorted mineralized conglomerate containing U-rich minerals and metal sulphides (Bruneton *et al.*, 2014). According to Bruneton et al. (2014), uranium and thorium are found in paleo quartz-pebble conglomerates the gold dominant Witwatersrand basin. The Witwatersrand Supergroup is overlain by the Ventersdorp Supergroup lavas (Robb *et al.*, 1997; Hobbs and Cobbing, 2007; Durand, 2012; Moshupya *et al.*, 2019), that are overlain by the discontinuous layer of the Transvaal Supergroup which encompasses the Black Reef Formation with an extraordinary amount of placer gold and these are denoted by conglomerates and quartzitic sandstones (Hobbs and Cobbing, 2007; Bruneton *et al.*, 2014; Fuchs *et al*., 2016 Moshupya *et al.*, 2019). Uranium forms next to the conglomerates where sedimentation occurs in the presence of carbon (Bruneton *et al.*, 2014). The Black Reef Formation is a basal layer of the Transvaal Supergroup and is formed from the sediments eroded from the Witwatersrand Supergroup that are associated with the Randian basement rocks of the Randian Era (3 to 2.75 Ga) (Hobbs and Cobbing, 2007; Durand, 2012). The Black Reef Formation is overlain by the Chuniespoort Group which consists of chemical and biochemical sediments, an example includes carbonates and banded ironstones (Durand, 2012). Below the Chuniespoort Group is the Malmani Subgroup (Hobbs and Cobbing, 2007; Durand, 2012) (See Figure 2) (Bruneton *et al.*, 2014).

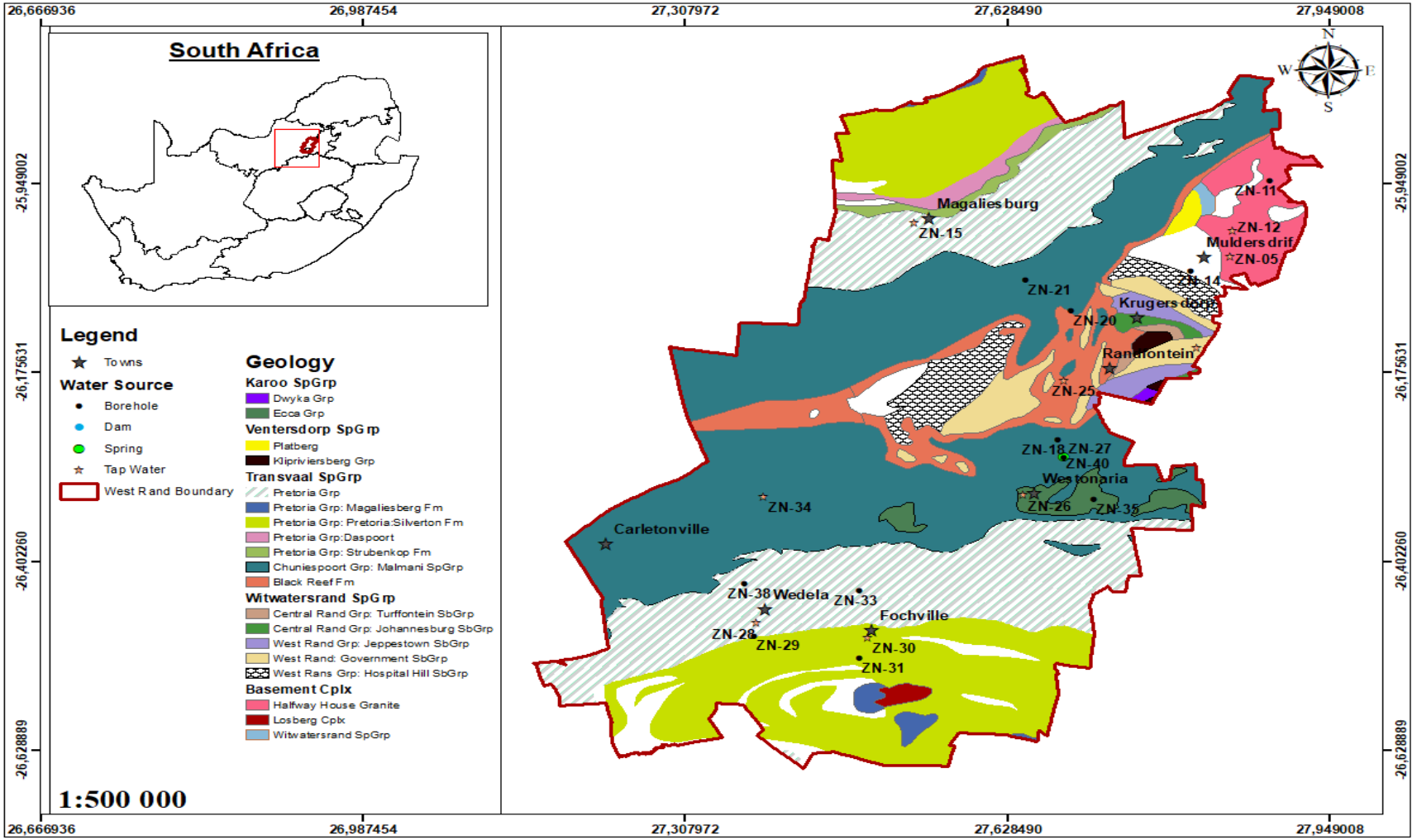

Figure 2: *A geological map of the West Rand (Modified from the Council of Geosciences).*

The study area is characterised by gently sloping and elongated ridges which control the hydrogeological setting in the region (Hobbs and Cobbing, 2007). The fractures, joints and faults found within the region serve as important features, which necessitate groundwater recharge and circulation of water within the West Rand region (Moshupya *et al*., 2019). Figure 3 shows that the West Rand region is dominated by karstic and fractured aquifers associated with the Malmani subgroup and Witwatersrand Supergroup respectively (Hobbs and Cobbing, 2007). The area of dolomitic and fractured rocks supports high groundwater productivity through cavities and fractures (Hobbs and Cobbing, 2007; Durand, 2012). The aquifers in this region have borehole yield ranges of >5.0 L/s for the karstic aquifer, 0.1 – 0.5 L/s for intergranular and fractured aquifers; and 0.5 – 2.0 L/s for fractured aquifers (Hobbs and Cobbing, 2007). The Magaliesburg area has a fractured aquifer with borehole yields of >5 L/s and is surrounded by fractured aquifers of lower borehole yields ranging from 0.5 to 5.0 L/s. Figure 3 also shows rivers, dams and wetlands. The wetlands are located between Randfontein and Westonaria, while the dams are located to the south of the study area. The Vaal dam is located outside of the study area and serves as a reference point as this is the source of the raw water used for the municipally supplied tap water within the study area.

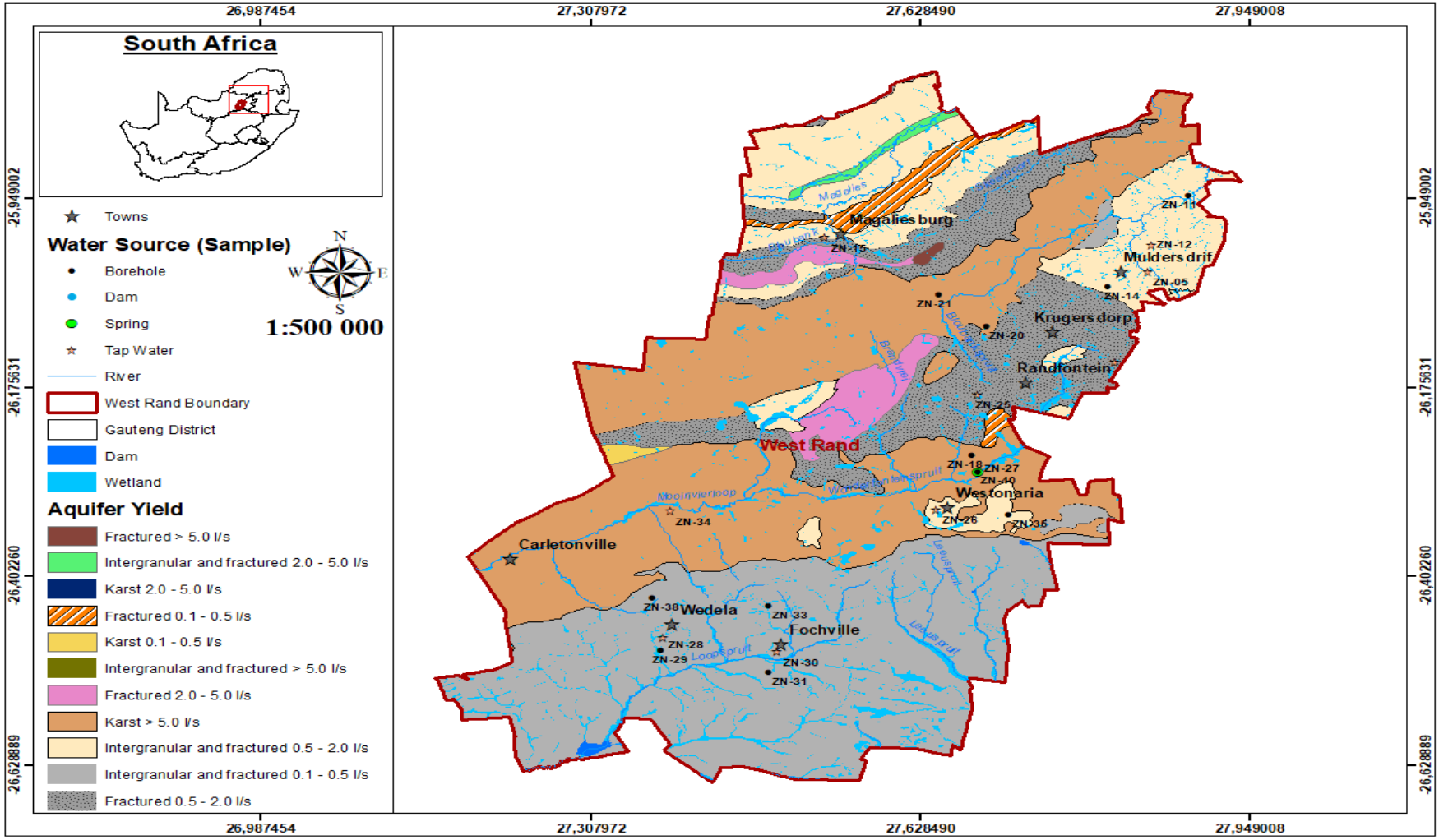

Figure 3: *A hydrogeological representation of the West Rand region (Modified from the Department of Water and Sanitation).*

Chapter 2: Literature review

2.1 The history of mining in South Africa

The Witwatersrand Basin was once a farming land that was sparsely populated, and this changed quickly after the discovery of gold (Tutu *et al.*, 2008). The area became densely populated and is now renowned for the gold that has been mined for several decades (Tutu *et al.*, 2008; Durand, 2012). They further explain that the discovery of the Main Reef was what led to the establishment of what is now known as the City of Gold, Johannesburg. This Reef was also discovered in smaller towns developed to the west and the east of Johannesburg (Tutu et al., 2008; Durand, 2012). More towns emerged as more discoveries of the Reef were made, and more mines were opened increasing the population of the mining towns (Tutu *et al*., 2008; Durand, 2012).

South Africa depends on mining to be economically competitive and for power generation from coal (Tutu *et al.*, 2008; Skipperud *et al.*, 2013). As important as mining is for South Africa, it poses a threat to the ecosystem. Mining exposes sulphide-rich rocks, pyrites and radionuclides which are susceptible to oxidation and transport (McCarthy, 2011; Madzivire et al., 2013). Gold is often found in trace amounts as well as in base-metal ores, particularly copper deposits (Vermaak, 2005; Godel et al., 2007; Durand, 2012; Kefeni et al., 2017). The mining of gold only focuses on the extraction of one metal rather than mining for polymetallic assemblages and thus a high volume of toxic waste is generated (Blowes *et al.*, 2003; Mhlongo and Amponsah-Dacosta, 2014). The geology in which gold appears predominantly contains pyrites and U (with its daughter radionuclides) which are the primary constituents of AMD (Madzivire *et al.*, 2013). The radionuclides are readily found in gold mine tailing dumps and may be introduced into groundwater once they encounter moisture sources or water (McCarthy, 2011; Madzivire *et al.*, 2013).

2.2 Acid mine drainage

2.2.1 The origin of AMD

Pyrite rich ores are the main contributors to AMD since they readily oxidize when exposed to oxygen, water and microorganisms (McCarthy, 2011; Luptáková *et al.*, 2015; Kefeni *et al.*, 2017). AMD is a process through which acidic water is produced when pyrite comes in contact with oxygen or oxygenated water (Durand, 2007; McCarthy, 2011; Luptáková *et al.*, 2015;

Kefeni *et al.*, 2017). The oxidation process occurs in two stages, the first stage producing sulphuric acid and ferrous sulphate, while the second stage producing ferric-hydroxide and sulphuric acid (Durand, 2007; McCarthy, 2011). This process occurs naturally and slowly when facilitated by weathering, it can, however, be catalysed by mining processes as well as naturally occurring bacteria (McCarthy, 2011; Luptáková *et al.*, 2015; Kefeni *et al.*, 2017). During the mining process, the overlying rock is broken down into smaller pieces which then allows for the faster generation of acid (McCarthy, 2011).

Since the acidification process is rapidly assisted by bacterial action, acidic water can dissolve and transport metals as well as radionuclides. The karstic environment in the West Rand region is threatened by the generation and introduction of AMD (Durand, 2007; McCarthy, 2011). The acidic water will react with the carbonate rocks and catalyze the formation of sinkholes and caves (Durand, 2007; McCarthy, 2011; Durand, 2012). The highly insoluble solids such as sulphates will then be carried in solution as undissolved solids suspended in water and eventually deposited in rivers, streams and groundwater (Akcil and Koldas, 2006; Tutu *et al.*, 2008; McCarthy, 2011; Kefeni *et al.*, 2017).

2.2.2 The effects of AMD on water quality

According to Rosner et al., (2001), the low pH of AMD necessitates the dissolution and migration of toxic metals. Some of these metals may remain suspended and, therefore, leach horizontally thereby polluting groundwater stored in the aquifer below mine tailings dams (Rosner *et al.*, 2001). Based on the geology of the region, AMD can undergo neutralization when it meets carbonate rocks causing the precipitation of some of these heavy metals and reducing their migration (Rosner, 1999). Through AMD and its chemistry, many heavy metals and radionuclides are mobilised, transported and leached into and out of various rock matrices which may have long term effects on the quality of water, fauna and flora in the surrounding areas (Cowart and Burnett, 1994, McCarthy, 2011, Huang, 2016).

2.3. Water quality

The importance of water cannot be stressed enough. It is one resource in which all reactions occur, hence, its importance. Emphasis must be put on the preservation of water as very little freshwater is available for use. With the growing population, the water demand is increasing exponentially and putting a strain on the available water resources. Groundwater is the main source of drinking water for most rural areas in West Rand (Duran, 2007). While gold mining in the region generates radioactive wastes which are dissolved and dispersed by flowing water

and eventually join streams, rivers, and groundwater resources (Durand, 2007). The growing urbanisation in the West Rand also means that more pressure will be exerted on the already stressed water resources and the sewer systems (Durand, 2007). Durand (2007) further explains that the growing population increases the risk of groundwater pollution and poses a threat to the quality of the water.

According to Durand (2007) and Dohare *et al.*, (2014) factors such as urbanisation, mining and waste mismanagement affect the quality of groundwater. The growing population has put a strain on freshwater resources. Groundwater is one of the resources that is quickly getting contaminated and depleted (Patil *et al*., 2012; Dohare *et al*., 2014).

Determining the make-up of groundwater is important and necessary to ensure that the water is suitable for the intended purpose (Dohare *et al.*, 2014). Any water of good quality has certain kinds of minerals to certify it fit for consumption and irrigation to sustain aquatic life. Groundwater must have some major and minor ions such as calcium, iron, nitrates, and some salts, and all these must be present in moderate amounts. In the case of groundwater, more salts may be present and this could be due to the interaction between the rocks, soil and the water or due to pollution (Dohare *et al*., 2014). Elevated nitrate levels suggest that there is some source of pollution usually in the form of sewage spillage, agricultural runoff and high chloride concentrations that may result from excess evaporation or seawater intrusion (Dohare *et al*., 2014).

Water quality must be closely and regularly monitored, and this is done through regular sampling and testing. According to studies conducted by Patil *et al.* (2012), groundwater depends on certain chemical reactions to govern its quality. Boreholes from farms in the West Rand region are regularly sampled by the Department of Water Affairs and Forestry to ensure that the water is contamination-free and safe for consumption (Durand, 2007). In the case that groundwater is contaminated, and the source of contamination can be pointed to a specific farm, the farmer must ensure that remediation is done. Karstic environments found within the West Rand region are highly endangered as they are indigenous to dolomitic rocks. The nature of dolomites threatens the quality of groundwater which is often utilized for drinking and for agriculture in the rural parts of the West Rand. Durand (2007) explains that the high permeability of dolomites renders karst environments endangered. This is because they form sinkholes and caves which make groundwater susceptible to contamination by pit latrines and other forms of waste (Durand, 2007). Groundwater systems and karstic environments are at

risk of contamination by AMD which may be transporting heavy metals and radionuclides. The AMD joins streams and ultimate permeates aquifers contaminating water that is usually used for drinking and irrigation. This contaminated water is then introduced and accumulates in animals and humans through drinking water and food, causing long term health problems (Ram *et al.*, 2021).

2.4 Radioactivity

Radionuclides are atoms with high mass numbers (Xiao and Laplante, 2004; Vermaak, 2005; Skipperud and Salbu, 2018). Atoms with mass numbers higher than 91 are considered unstable; and are, therefore, radioactive (Vermaak, 2005). Radioactivity can be defined as the decay of unstable atomic nuclei to attain a more stable configuration (Xiao and Laplante, 2004; Vermaak, 2005; Madzivire *et al.*, 2014; Skipperud and Salbu, 2018). They gain stability by emitting radiation particles such as alpha, beta or gamma radiation (Xiao and Laplante, 2004; Vermaak, 2005; Madzivire *et al.*, 2014; Skipperud and Salbu, 2018). When an unstable nucleus loses protons and two neutrons, alpha particles are formed. Alpha emissions are also known as Helium emissions (Xiao and Laplante, 2004; Vermaak, 2005; Skipperud and Salbu, 2018). The reaction below is an example of alpha emission:

$$^{238}_{92}U \longrightarrow {}^{234}_{90}Th + {}^{4}_{2}\alpha$$

The loss of an electron from a nucleus results in the formation of beta particles (Xiao and Laplante, 2004; Vermaak, 2005; Skipperud and Salbu, 2018). The emission of a beta particle is illustrated by the reaction below:

$$^{228}_{88}Ra \longrightarrow {}^{228}_{89}Ac + {}^{0}_{-1}e$$

The emission of alpha and beta particles leaves the nucleus of the newly formed daughter nuclide in an excited state (Vermaak, 2005). The nucleus of the daughter nuclide moves from this excited state to the ground state releasing the excess energy in the form of photons, this photon is known as gamma-ray emission (Xiao and Laplante, 2004; Vermaak, 2005; Skipperud and Salbu, 2018). A gamma emission reaction is illustrated below:

$$^{234}_{90}Th \longrightarrow {}^{234}_{91}Pa + {}^{0}_{-1}e + {}^{0}_{0}\gamma$$

Radioactive elements are those elements that naturally emit ionizing radiation and this ionizing radiation can be used to characterize different elements (Xiao and Laplante, 2004; Vermaak, 2005; Skipperud and Salbu, 2018).

2.4.1 Radionuclides

2.4.1.1 The origin of radionuclides

Earth contains both natural and pseudo radionuclides (Milenkovic *et al.*, 2019). NORMs such as ^{238}U, ^{232}Th and ^{40}K have been on the surface of the Earth since its formation (Faanu et al., 2011; IAEA, 2011; Milenkovic *et al.*, 2019). Pseudo radionuclides are produced synthetically in the laboratory while some form because of the decay of the NORMs (Faanu *et al.*, 2011; Skipperud and Salbu, 2018; Milenkovic *et al*., 2019). Pseudo radionuclides do not exist in nature, but they were brought into the environment by atmospheric nuclear weapons testing and nuclear accidents an example is ^{137}Cs (Skipperud and Salbu, 2018).

2.4.1.2 NORMs

NORMs are found readily on the surface of the Earth and may be classified into two groups: terrestrial NORMs and cosmogenic radiation (Madzivire *et al.*, 2014; Magagula, 2015; Skipperud and Salbu, 2018). Terrestrial NORMS are materials that are found on the Earth's crust and mantle while cosmogenic radiation originates from cosmic rays and reactions between some gases in the Earth's atmosphere (Madzivire *et al.*, 2014; Magagula, 2015; Skipperud and Salbu, 2018). Although NORMs are considered naturally occurring, human activities also contribute to the elevated levels of radionuclides in the atmosphere (Madzivire *et al.*, 2014; Magagula, 2015).

2.4.1.3 Decay series

A decay series is a chain, which consists of different products that a radionuclide forms as it decays (IAEA, 2011). When an unstable nucleus disintegrates it forms a product which is called the daughter nucleus. If the newly formed daughter nucleus is unstable, it will continue to decay until it reaches a stable configuration. As this process continues, a decay chain/ series is formed. There are three known decay series and those are the Uranium decay series, the Thorium decay series as well as the Actinide decay series (Faanu *et al.*, 2011) (Refer to Figure 4). Each decay chain is dependent on the half-life of elements. The half- life is known as the time it takes for half of a radionuclide to decay into its daughter nuclides/ products (Madzivire *et al.*, 2014).

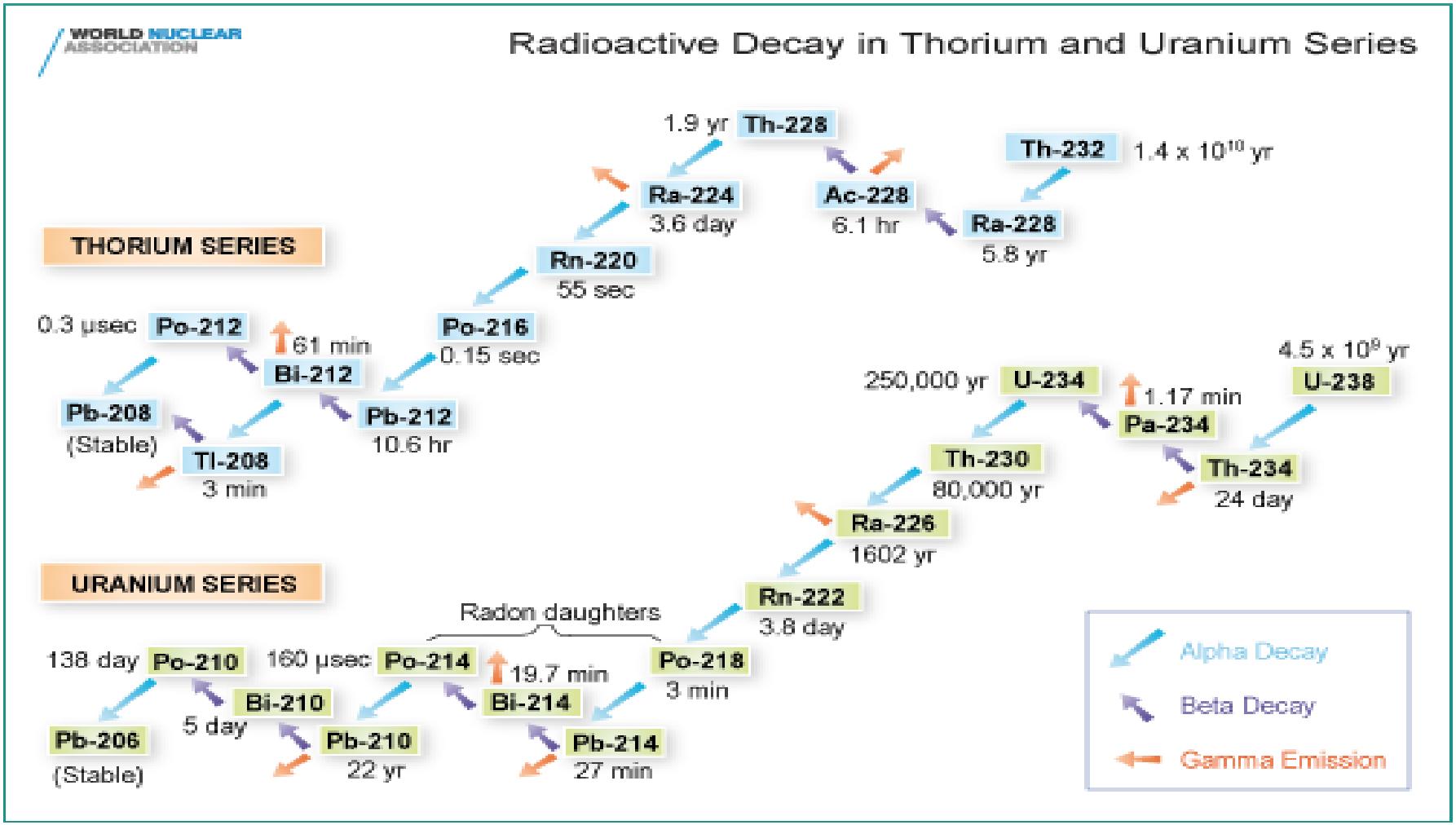

Figure 4: *An image illustrating the uranium and thorium decay series (source: World Nuclear Association, 2019).*

2.4.2 The chemistry of elements

This study focused on radionuclides such as U, Th, Ra and Pb; and will therefore only focus on the chemistry of these elements. According to Milenkovic *et al.* (2019), the geology of an area is responsible for determining the concentration of radionuclides. They further explain that some NORMs can be associated with certain rock types and, therefore, influence the distribution and migration of radionuclides. According to Pedrobom *et al.* (2017), chemical speciation has a pivotal role in the distribution of radionuclides in the environment and can be used to predict the solubility of radionuclides and hence, the rate at which these radionuclides may leach into the groundwater. Pedrobom *et al.*, (2017) and Winde (2015) describe speciation as the form of a chemical substance. The speciation of radionuclides is very important in the mobilization and absorption of biological molecules (Skipperud *et al.*, 2013; Winde, 2015). Skipperud *et al.* (2013) and Winde (2015) attribute that the speciation of radionuclides depends on a few factors such as their source, the transport mechanisms as well as the physicochemical parameters readily provided by the environment. For some of the radionuclides to travel far and fast they may need to form complexes with some ions or complexing ligands (Tutu *et al.*, 2009; Skipperud *et al.*, 2013; Neiva *et al*., 2019).

The distribution of radionuclides is a function of their chemistry (Neiva *et al*., 2019). Neiva *et al.* (2019) add that the pH of the water in which these radionuclides are carried also influences their distribution. A low pH may cause the radionuclide to dissolve and thus be bio-available for transport, the liquid phase necessitates the migration and transportation of these radionuclides further away from the source.

2.4.2.1 The chemistry of uranium

The known oxidation states of Uranium are +2, +3, +4, +5 and +6 with +4 and +6 being the most stable valence (Vermaak, 2005; Neiva *et al*., 2019). The uranium (IV) oxidation state is commonly found as a highly insoluble species in the environment (Vermaak, 2005; Tutu et al., 2009; Neiva *et al*., 2019). It is for this reason that uranium (IV) is less mobile than uranium (VI) (Vermaak, 2005; Skipperud *et al*., 2013; Neiva *et al*., 2019). According to Neiva et al. (2019) uranium is most active in the oxidation states +4 and +6. They further explain that the uranium will react with oxygen to form uranyl ions or uranium dioxide, which are highly soluble in groundwater under anaerobic conditions.

There are various conditions under which U may exist and it will behave differently under these conditions (Neiva *et al*., 2019). U (VI) is formed when U(IV) is oxidized and this results in the

formation of complexes with ions such as OH^-, F^-, Cl^-, CO_3^{2-}, SO_4^{2-} and PO_4^{3-}; and other complexing ligands such as EDTA, thereby increasing its mobility (Tutu *et al*., 2009; Neiva *et al*., 2019). This process occurs under acidic conditions (Tutu et al., 2009; Neiva et al., 2019). Uranyl ions present in secondary U minerals such as autunite (hydrated calcium uranyl phosphate) are relatively stable under acidic conditions as illustrated in Figure 5b (Tutu et al., 2009; Huang, 2016; Neiva *et al*., 2019). Under alkaline and neutral conditions, the carbonate compounds will form, causing salt formation and reducing the mobility of the U and its associated minerals (Vercouter *et al*., 2015; Antunes *et al*., 2018; Neiva *et al*., 2019). These reactions can be better explained using the Eh-pH diagram which shows the various conditions under which U can exist (Huang, 2016). The solid regions of the Eh-pH diagram show fields of stability while the lines show regions where compounds may coexist (Huang, 2016).

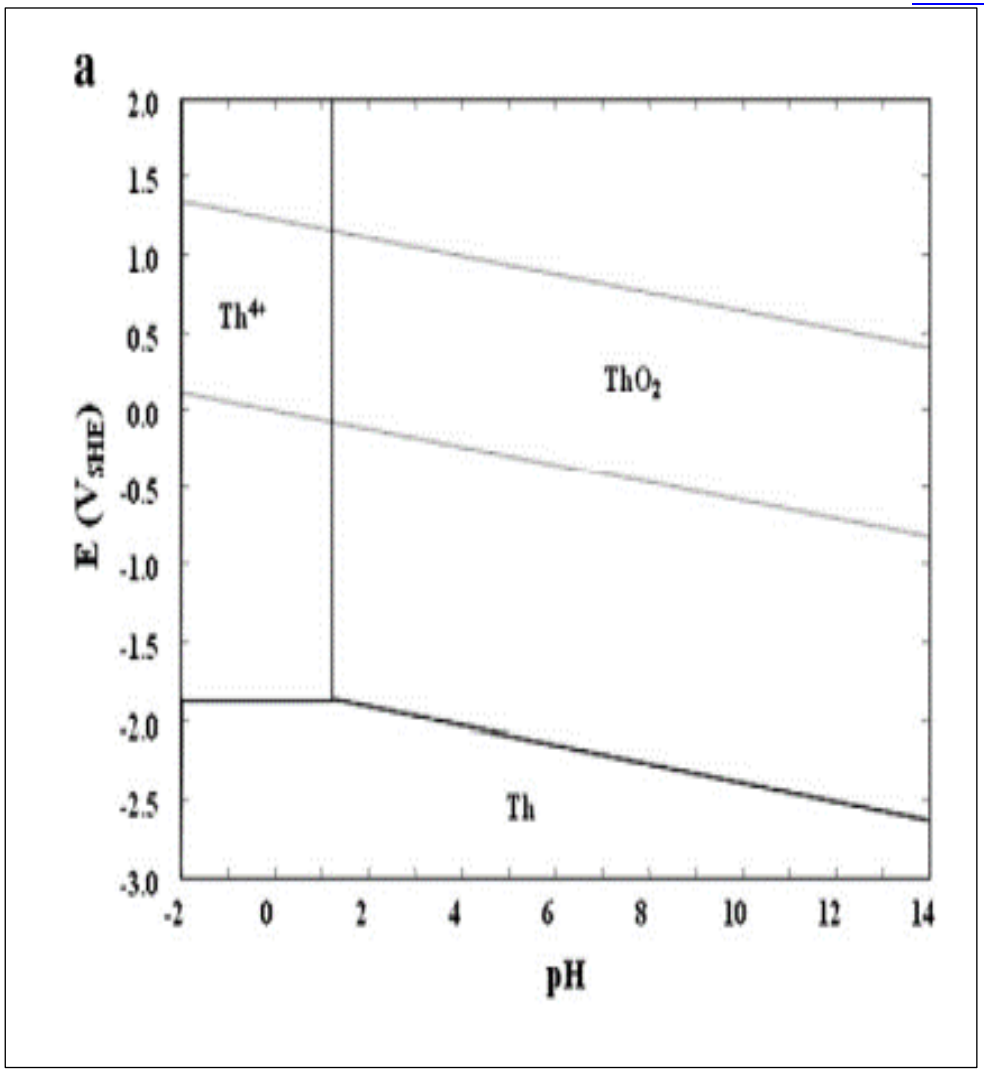

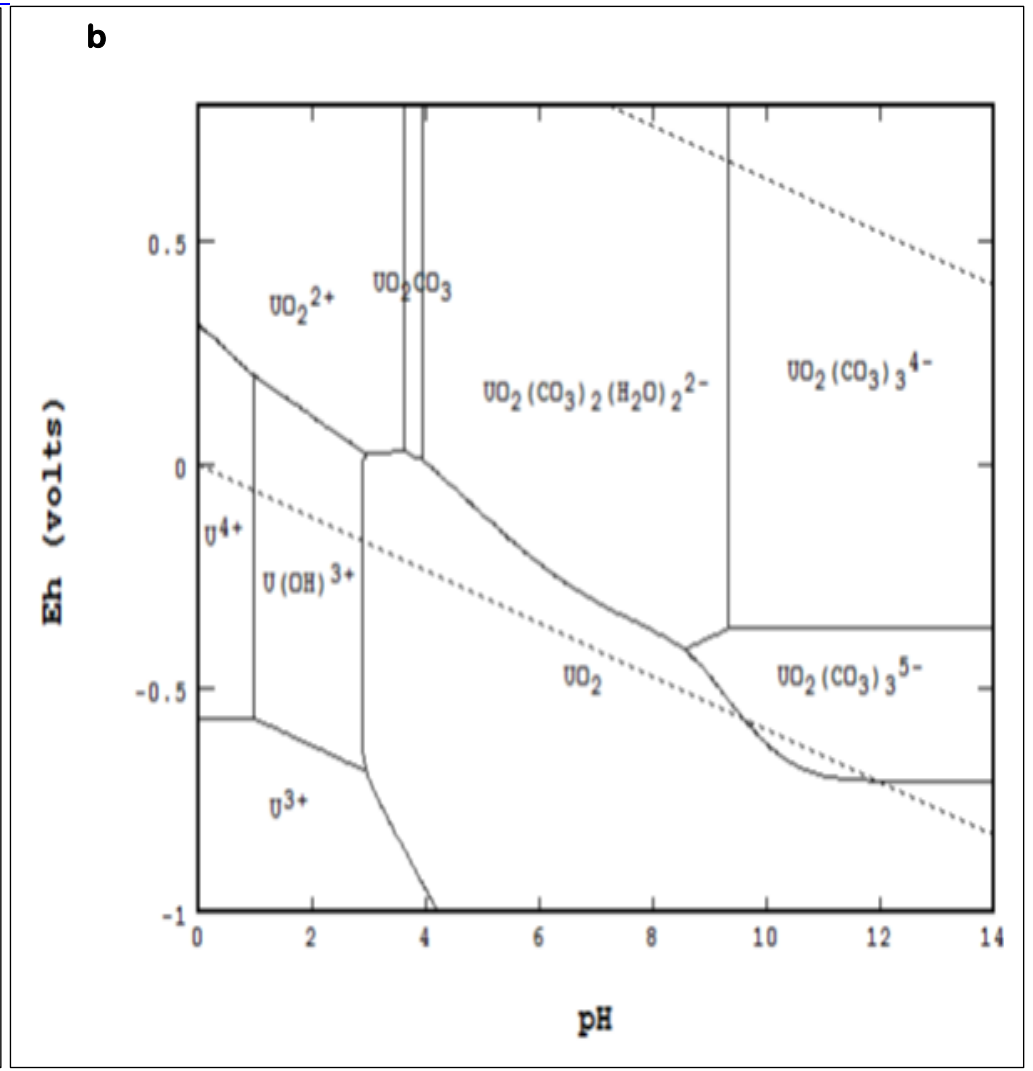

Figure 5: *An Eh-pH diagram showing the stability condition of (a) Th and (b) U (Kim and Osseo-Asare, 2012; Huang, 2016).*

2.4.2.2 The chemistry of thorium

Thorium (Th) is the product that forms during the decay of ^{234}U and also exists naturally in the Earth's crust. It is less soluble and hence, is less mobile as compared to U (Neiva *et al*., 2019). Neiva *et al.* (2019) further state that the complexes formed by Th can readily precipitate out when the pH rises above 5 and it is due to this reason that it may be absent in liquids. In acidic to neutral pH, Th exists as ThO_2 (see Figure 4) (Kim and Osseo-Asare, 2012). Studies done by Neiva *et al.* (2019) suggest that Th usually forms carbonate hydroxide complexes which can be used to explain their insolubility (see Figure 5a). The extent of contamination by radionuclides depends on their mobilization (Boekhout *et al*., 2015). The mobile radionuclides travel further and fast, and thus may easily be absorbed by biological molecules (Boekhout *et al*., 2015).

2.4.2.3 The chemistry of radium

Radium (Ra) forms part of the alkali Earth metals on the periodic table and it is also the heaviest element in the group (Tsezos and Keller, 1983). It has a half-life of 1620 years which suggests that it can be available on the Earth's crust for several years at a time (Tsezos and Keller, 1983). Alam *et al*. (1999) further explain that the abundance of Ra is governed by the geology of an area, hence, different areas will have varying concentrations of Ra. According to Alam *et al*. (1999), Ra exhibits similar chemical behaviour as calcium. Studies done by Tsezos and Keller (1983) suggest that neutral to alkaline pH (ranging from 7 – 10) is the optimum pH at which Ra may be removed through biosorption. At low pH ranges Ra can interact with certain types of biomasses thereby making it available for removal from solution (Rosner, 1999). Based on the study conducted by Rosner et al. (2001) ^{226}Ra can migrate from rocks with the help of groundwater and is retarded by clay minerals. ^{226}Ra forms insoluble precipitates such as $RaCO_3$ and $RaSO_4$ when it enters shallow groundwater or meets surfaces containing carbonates or sulphates (Rosner *et al.*, 2001). According to Alam *et al.* (1999), ^{226}Ra which is dissolved in water is 40 times more harmful than ^{90}Sr since its long half-life enables it to accumulate in the human body.

2.4.2.4 The chemistry of lead

Lead (Pb) is dense, naturally occurring heavy metal which usually appears in trace amounts in hydrothermal ores as PbS and ores containing sulphides (Wu *et al.*, 2019; Ram *et al.*, 2021). Pb is formed from the decay of uranium and thorium and it has a half-life of 22 years (see figure 4) (Yoon *et al.*, 2013; Ram *et al.*, 2021). Pb is toxic once ingested or inhaled and must

therefore be monitored as it can result in death if absorbed into the blood stream (Shahid *et al.*, 2012; Yoon *et al.*, 2013; Wu *et al.*, 2019). According to Shahid *et al.* (2012), Pb behaves differently under different conditions. Shahid *et al.* (2012) and Ram *et al.* (2021) further explain that Pb^{2+} appears as a free ion which thrives under acidic conditions due to its occurrence in sulphide-rich ores. Under alkaline conditions the free Pb^{2+} free ion binds with a hydroxyl (OH) molecule to form a Pb-OH molecule which is stable under these conditions (Shahid *et al.*, 2012; Ram *et al.*, 2021). The study conducted by Shahid *et al.* (2012) has shown that Pb can interact and bind with chelating ligands such as EDTA, citric acid (CA) and fulvic acid (FA) lowering the pH of the water and thereby increasing its mobility. Out of all the chelating ligands, EDTA has been proven to easily scavenge Pb from soils and rocks, therefore, increasing its mobility (Shahid *et al.*, 2012). The addition of carbonates increases the pH of the solution and causes the Pb to form insoluble precipitates (Ram *et al.*, 2021).

2.4.3 The mobility of radionuclides

Radionuclides behave differently and this is mainly due to their origin as well as their chemical speciation (Faanu *et al*., 2011; Milenkovic *et al*., 2019). Many factors influence the mobility of radionuclides such as chemical speciation, pH, the chemistry of the transport and waste, as well as the mode of transport (Faanu *et al*., 2011; IAEA, 2011). The chemistry of the transport mechanism, water, in this case, is of particular importance as the water may contain ions or organic and inorganic matter which has the potential to mobilise radionuclides (IAEA, 2011). The radionuclides are then carried in solution and may get distributed to various areas or contaminate the groundwater system because of leaching (IAEA, 2011). The speciation of radionuclides not only affects the mobility of radionuclides but also the fixing of these radionuclides onto the rock matrix provided the conditions are favourable (Kim and Osseo-Asare, 2012; Huang, 2016).

Leaching can be described as the process of extracting materials from their hosts (Koliabina, 2018). The phenomenon explained above can be used to explain how waste from acid mine dumps is carried into streams and the surrounding mining communities (Geletneky *et al*., 2005). Leaching depends on the availability of water in the soil, the greater the amount of water, the greater the risk of leaching (Koliabina, 2018). Another factor that governs the leaching of radionuclides in the soil is their oxidation state, for example, Uranium (IV) is relatively insoluble and may not easily leach into the groundwater (Vermaak, 2005; Geletneky *et al*., 2005).

Moreover, the existence of radionuclides in groundwater is intensely affected by the flow of systems and their geochemical characteristics (Marshak, 2011). Parts of diverse hydraulic regimes recharge, through flow and discharge even within the same aquifer are influenced by differences in the geochemical environment (Marshak, 2011). The geochemical environment refers to the chemical gradient that is created when the minerals are dissolved in the moving water (Marshak, 2011).

2.5 Acceptable radiological levels in drinking water

When water quality tests are being conducted there must be a reference point as to what acceptable levels of chemicals are permissible in the water used for various purposes. The background level of radionuclides is by far the most important water quality parameter to consider especially near mines. The West Rand region is one such areas that has many operational and closed mines. Through this mining activity, many minerals and radionuclides are exposed and mobilised which then make their way to streams and ultimately end up in drinking water systems (EPA, 2001; WHO, 2011). However, there are some NORMs, which are found readily on the Earth's crust.

The primitive existence of NORMs in the Earth's crust and the mining activities taking place in the West Rand region require background tests to be done to account for the radionuclides which may already be present in the water. The purpose of this background check is to establish the concentration and type of the radionuclides present in the water, identify the radiological characteristics of the source of the water and assess the extent to which the radionuclides are diffused in the water (WHO, 2011). One way in which the concentration of radionuclides can be checked is through the screening of drinking water for gross alpha-beta activities (DWAF, 1996; WHO, 2011). The World Health Organisation (2011) and the Department of Water Affairs and Forestry (1996) further explain that the screening for radionuclides must be done regularly, and the gross alpha and gross bet activities may not exceed 0.5Bq/L and 1Bq/L, respectively.

According to the World Health Organisation (2011), the presence of NORMs in drinking water should not be a problem if their concentration is below the established guideline value. The World Health Organisation (2011) suggests that NORMs are more likely to give higher radiation doses in water as compared to artificial radionuclides. The guideline states that the Individual Dose Criterion (IDC) should not exceed 0.1mSv/year (DWAF, 1996; WHO, 2011). The IDC is a set of rules that have been put in place to ensure minimum radiation exposure and

hence, reduce the health-related issues following exposure (EPA, 2001; WHO, 2011). In addition to screening, water guidance levels must be adhered to. The water guidance levels assess the rate of consumption of radionuclides in 2L/day for a year (WHO, 2011).

If the screening and the guidance levels yield activities that are higher than normal, then further tests must be done to determine the individual radionuclides present in the water and their respective concentrations. The allowed amount of radiation exposure from a single source is 0.25mSv/yr (Protection and Measurements, 1954; Winde, 2015). ^{226}Ra has the lowest permissible activity concentration in drinking water of 0.148 Bq/L (DWAF, 1996; European Commission, 1998; WHO, 2011). The World Health Organisation (2011) has set a U limit of 30µg/L in drinking water.

Studies show that Portugal (Europe) has set the allowed activity of ^{3}H in drinking water to 100 Bq/L as per the WHO guidelines (European Commission, 1998; Madruga *et al*., 2009; WHO, 2011). The TDS acceptable limits have been set at 600 mg/L for palatable drinking water and anything more than this would render the water unsuitable for drinking (WHO, 2011). Another important water quality parameter to consider is pH. The pH of drinking water must fall within the range of 6.5-8.5 (Forestry, 1996). Water with a pH less than the range would be considered acidic, while a higher pH would qualify the water to be basic (WHO, 2011). The DWAF (1996) have adopted the WHO (2011) drinking water guidelines as the recommended limits for South African domestic water quality.

2.6 Radioactivity in drinking water

2.6.1 South Africa

According to Winde (2015), two surveys were conducted to investigate radioactive pollution in rivers due to gold mining in the Witwatersrand Basin. The first study found that the radioactive pollution in rivers was high while the second study reported very high U levels in the Witwatersrand Basin and the urine of mine workers (Winde, 2015). Another study was conducted for U and ^{226}Ra pollution in soil and water to determine the concentration and understand the behaviour and migration of these radionuclides within the ecosystem. This was achieved by collecting samples from various vegetables (both inland and aquatic), cow tissue, milk and dung, fish, and some waterbirds (Winde, 2015). Calculations of the effective dose yielded results below the allowed amount of 0.25 mSv/yr for all the exposure pathways (Winde, 2015). To understand the migration of U, another study was conducted in uncontaminated

streams and groundwater bodies around the country (Winde, 2015). This study, however, did not yield tangible results (Winde, 2015).

According to Madzivire *et al.* (2013), gold mining has resulted in elevated concentrations of radioactive materials in water. This study focused on the radioactivity of mine water and how it affects portable water. The gross-α and gross-β activity concentrations reported in this study were approximately six times higher than the acceptable WHO (2011) drinking water guidelines (Madzivire *et al.*, 2013). and thus facilitated the need for the analysis and identification of the radionuclides present in the samples. Only ^{234}U reported activity concentrations that were four times higher than the allowed limit. The acidic pH of the water which was below 5 coupled with the elevated ^{234}U activity concentrations suggests that the water is not safe for consumption or irrigation (Madzivire *et al.*, 2013).

Madzunya *et al.* (2020) conducted a study in the West Rand region and the Modiri Molema Municipality (North-West Province) to assess the radiological health risks of drinking water and soil dust. All drinking water guidelines state that the gross-α and gross-β activity concentrations should be measured first before any other tests may be done. The gross-α and gross-β activity concentrations from this study were below the acceptable limits set by WHO and DWAF so no further tests were conducted (Madzunya *et al.*, 2020).

Most of the mine tailings found across the West Rand region threaten the health of people living near them (Moshupya, 2021). A study conducted by Moshupya (2021) reported activity concentrations of 0.69 Bq/L and 0.15 Bq/L for ^{238}U and ^{232}Th in water samples, respectively. However, the samples collected from the tailings and soils near the tailings reported very high activity concentrations which were in some cases, 10 times higher than the acceptable amount (Moshupya, 2021). The effective dose was 3 times higher than the allowed public radiation exposure limit of 1 mSv/yr, which suggests that the public is at risk due to the radiation exposure (Moshupya, 2021)(See Figure 6).

A study conducted in the rural Pofadder of the Northern Cape found that the groundwater in the region had been contaminated with U by 9x more than the tolerable daily intake (Winde *et al.*, 2017). The Pofadder region is located approximately 50 km away from the Aggeneys mine which is rich in trace metals like copper (Cu), lead (Pb) and zinc (Zn) (Winde *et al.*, 2017). This study suggests that the high U concentration was a result of the leaching of elements from the geology of the area from the rock-water interaction and water eventually recharges the aquifers in the area (Winde, 2015; Winde *et al.*, 2017).

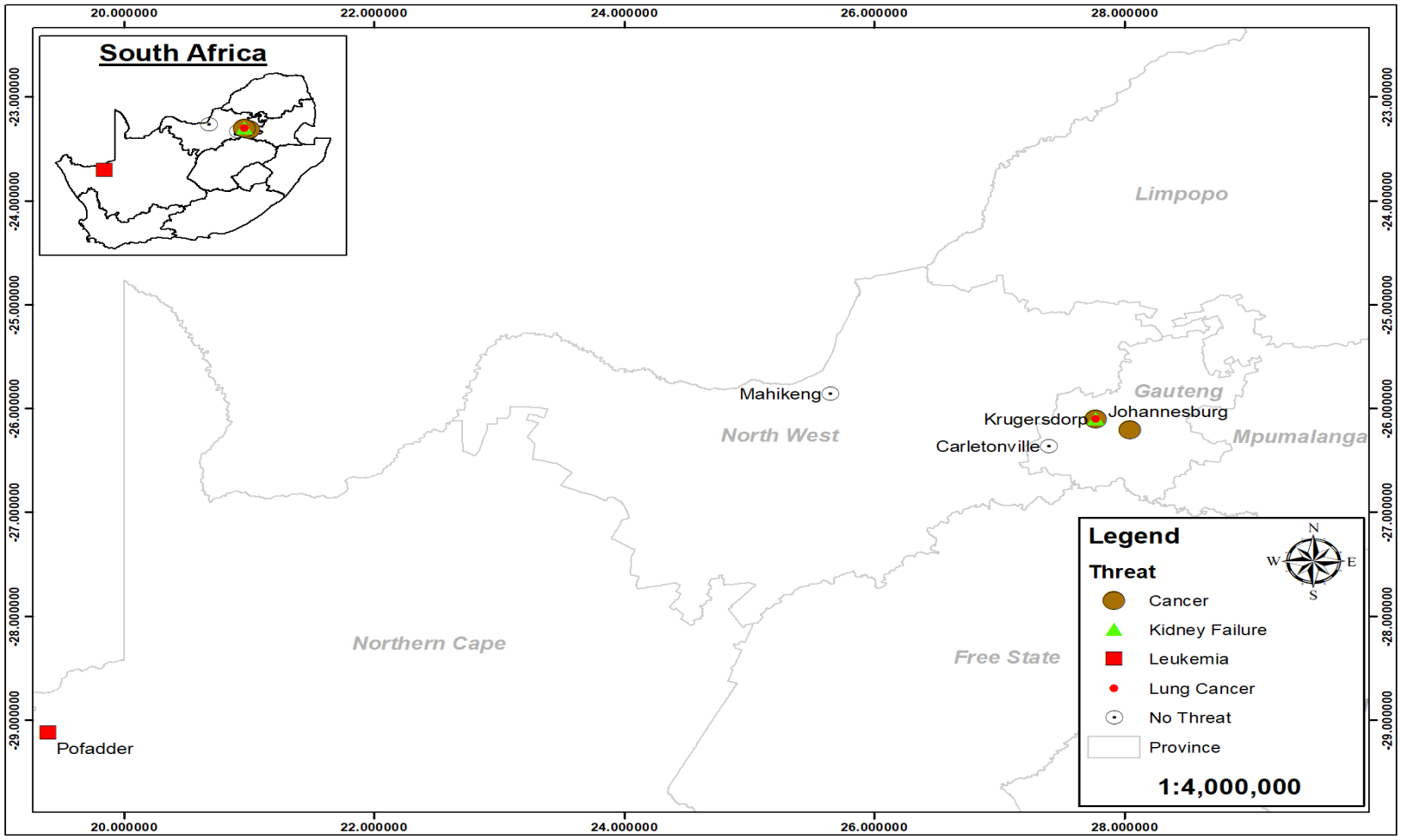

Figure 6: *A map showing the locations of previous studies and threats associated with the findings of those studies.*

2.6.2 Other parts of the world

Several studies were conducted across the world to better understand the recharge and flow dynamics of groundwater and how groundwater impacts the economy of a country. This has been achieved with the use of isotopes, both stable and radioactive.

An earlier study by Alam *et al*. (1999) in Bangladesh was aimed at conducting a radiological assessment of drinking water in the Chittagong region. The study suggests that groundwater has high concentrations of NORMs. Alam *et al*., (1999) found the mean activity concentrations of ^{222}Rn, ^{226}Ra, ^{232}Th and ^{40}K to be 4.46 Bq/L, 0.043Bq/L, 0.19Bq/L and 4.16Bq/L respectively for drinking water samples. No ^{134}Cs or ^{137}Cs was present in the samples (Alam *et al*., 1999). The calculated effective dose because of water consumption was 56.2 mSv/yr, 7.6mSv/yr and 16.7mSv for ^{232}Th, ^{226}Ra and ^{40}K, respectively.

A study to deduce the amount of ^{3}H in numerous sources of water such as rivers, streams, rain, and groundwater was conducted in Serbia. This study focused on areas near nuclear research sites and compared three methods for the detection of ^{3}H in water. The three methods used were electrolytic enrichment, direct measurement and the samples prepared by the sample oxidizer (Nikolov *et al*., 2013). The study conducted in Serbia found ^{3}H levels in water to be within the allowed amount and the three methods also yielded results, which coincided with one another (Nikolov *et al*., 2013). Nikolov *et al.* (2013) recommend that the isotopic enrichment method be used for investigating ^{3}H in groundwater. Portugal has conducted a similar study on ^{3}H in groundwater and found the levels to be within the allowed limits (European Commission, 1998; Madruga *et al*., 2009).

Coal mining in Croatia has resulted in the introduction of heavy metals as well as radionuclides and has threatened freshwater resources (Medunić *et al*., 2020). Rasa coal is renowned for its high radioactivity of 500-1200 Bq/kg in the 1970s and 250-300 Bq/kg in the 1980s, ten times more than other coal types in the world (Medunić *et al*., 2020). They further state that China also reported high U activities. The Croatian study established that the chemical weathering of the Rasa Croatian coal by groundwater is causing harm to the environment in the area (Medunić *et al*., 2020). The results of the study showed that Rasa coal mining has affected the water quality in the region and increased levels of U, Molybdenum (Mo) and Vanadium (V) were reported (Medunić *et al*., 2020).

A study of the radiological safety of groundwater was conducted in Namibia (Mathuthu *et al.*, 2021). Namibia is one of the U-rich countries where U is mined in its purest form. This study reported higher (20 times) activity concentrations of U while those of Th were below 1 (Mathuthu *et al.*, 2021). The only explanation for these elevated U activity concentrations is the geology of the area (Mathuthu *et al.*, 2021).

2.7 Health implications associated with radiation exposure

All living organisms are affected by radiation in some way. For this study, it is important to focus on radiation exposure in human beings. Humans are exposed to ionising radiation by ingesting, inhaling, or absorbing the ionising particles of radiation through the skin (Mathuthu *et al.*, 2021). According to Madzivire *et al.* (2014), terrestrial NORMs are primordial and readily available on the Earth's crust increasing human exposure to ionising radiation. These terrestrial NORMs get dissolved and mobilized by water, get absorbed by plants through the soil and eventually get ingested by human beings through vegetables or meat from livestock or fish (Durand, 2007; Mathuthu *et al*., 2021). The radionuclides have long half-lives and may thus build up inside the human body causing long term exposure to ionising radiation (Durand, 2007; Mathuthu *et al*., 2021). Outside the body, alpha particles can be stopped by the skin but once ingested or inhaled, these can induce double strand breaks in DNA rendering the DNA unable to repair itself causing cells to divide irregularly (Durand, 2007). Cells that divide irregularly may result in various illnesses such as paralysis or cancer (Durand, 2007). Studies done by Mathuthu *et al.* (2021) and Durand (2007) suggest that the ingestion of alpha- and beta-emitting radionuclides may result in kidney failure, blindness and different kinds of cancers depending on where the radionuclides accumulate. The alpha- and beta-emitting radionuclides such as U, Th, Ra and Pb can also cause tissue damage and eventually burns if highly concentrated (Durand, 2007; Madzivire *et al.*, 2014).

Chapter 3: Materials and Methods

3.1 Sampling

3.1.1 Site selection

The West Rand region has been selected strategically due to more than a century's worth of gold mining activity. To achieve this, a desktop study was conducted to identify the major towns, their population densities, mining sites and land use. These parameters were sorted in order from towns with the highest population densities to towns with the dominant land use being mining. High population densities suggest that more people are at risk of getting exposed to radioactive materials produced from gold mining activities which are dominant in the West Rand region. The coordinates of the selected sites shown in figure 1 were compiled before the field investigations and used during sample collection.

3.1.2 Sampling

23 water samples were collected using 1L polyethene bottles. From the 23 samples collected, 1 sample was from surface water (Vaal dam), 8 were tap water samples and 12 were groundwater samples with 6 sampled directly from boreholes for tritium analysis. The polyethene bottles and caps were washed out twice with the sample before sampling (as shown in figures 7a and 7b) and then sealed. Boreholes were purged for 3-5 minutes before the sample was collected to allow the water which was within the pipes to flow out before collection (Figure 7c). The samples were collected in duplicates and additional tritium samples were collected in areas where the groundwater was sampled directly from the borehole. The samples were then labelled correctly using a permanent marker and transported to the laboratory for storage. Physico-chemical variables such as pH, TDS and temperature were measured in situ during sample collection (see figure 7d). To assess the quality of water one must investigate the chemical parameters. Chemical parameters are limits that are set to assess the quality of products, in this case, the quality of water (Islam *et al*., 2017). Patil *et al.* (2012) highlight the importance of testing and assessing water before it can be considered safe for use There are various parameters to test before assigning a purpose for the water and these are selected based on the intended purpose (Patil et al., 2012; Dohare *et al*., 2014). All these parameters are important in ensuring that the water is of a good standard for drinking. These parameters can be used to indicate changes in water quality (Islam *et al*., 2017). For example, high TDS may indicate that there is an elevated amount of ions or particles in solution which suggests that the

water may not be safe to drink (Islam *et al*., 2017; Serrano-Finetti *et al*., 2019). Both the physical and chemical parameters are important in determining the quality and purity of water (Patil *et al*., 2012). The samples were then transported to the NNR laboratory for radionuclide analysis.



Figure 7: *Images showing sample collection (a) Vaal dam sample collection, (b) sample collection at a spring, (c) purging of pipes linked to borehole before sample collection and, (d) taking physico-chemical parameters in situ.*

3.2 Sample analysis

3.2.1 Tritium analysis

The samples collected for tritium analysis were distilled and then concentrated by electrolysis. The electrolytic cell contains two concentric metal tubes that are isolated from each other. The outer anode is also a container, made of stainless steel. The inner cathode is made of mild steel with a special surface coating. 500 ml was distilled, and some sodium hydroxide was added to it. This distilled sample containing sodium hydroxide was phased into the cell. A direct current ranging between 10 A and 20 A was passed through the cell. The cell is cooled due to the heat generated. After a few days, the amount of electrolyte is reduced to 20 ml. The volume of the electrolyte was reduced by a factor of 25x corresponding to tritium enrichment of about 20. Samples of standard known tritium concentration (spike) were run in one cell of every lot to confirm the enrichment achieved. Samples were prepared for liquid scintillation counting by distilling concentrated water samples directly from the highly concentrated electrolyte. Exactly 10 ml of distilled water sample was mixed with 11 ml of Ultima Gold and placed in a vial of the analyser. The samples were then counted in 2-3 cycles for 4 hours. Samples were analysed at iThemba Labs Gauteng and results were reported in TU. The detection limit for concentrated samples is 0.2 TU. The results were then converted to mBq/L using the following conversion factor:

1TU =11.8 mBq/L

The residence times were calculated using equation 1 (Clark and Fritz, 2013):

$t = -17.93 \ln \left(\frac{At\ 3H}{Ao\ 3H}\right)$ *(Equation 1)*

where:

t = mean residence time (MRT) in years

A_t = residual activity remaining after decay time

A_0 = initial ^3H activity.

The ^3H activity in the sampled rainfall (Abiye *et al*., 2015) was used as the initial ^3H activity.

3.2.2 Stable isotope analysis

Stable isotopes $\delta^{18}O$ and $\delta^{2}H$ were analysed at the University of Witwatersrand, South Africa, using the Liquid Water Isotope Analyzer (LIWA) Model 45EP. The LIWA uses high-resolution laser absorption spectroscopy to provide accurate isotope ratio measurements over a wide range of delta values (that is, from highly depleted to highly concentrated states). This equipment is comprised of a laser analysis system and an internal computer, an automatic liquid sampler, a small diaphragm vacuum pump, and a room air suction line that removes moisture by passing air through a Drierite column. A 0.75 µl sample was injected from the PTFE septum into the autosampler using a Hamilton microliter syringe. The autosampler inlet is heated to 46 ° C to accelerate the evaporation of the sample under vacuum immediately after injection. The vapour then travels down the transfer line into the pre-evacuated mirrored chamber for analysis. A 1 ml aliquot of a sample was pipetted into a 2mL automated sampling glass vial and closed with PTFE septum caps. Five standards were utilized in the analysis procedure where the laser machine automatically calibrated itself and measured stable isotope values. The standards used are 5C: $\delta^{2}H$ 9.2 ± 0.5, $\delta^{18}O$ 2.69 ± 0.15‰, 4C: $\delta^{2}H$ 51.6 ± 0.5 ‰, $\delta^{18}O$ 7.94 ± 0.15 ‰, 3C: $\delta^{2}H$ 97.3 ± 0.5‰, $\delta^{18}O$ 13.39 ± 0.15‰, 2C: $\delta^{2}H$ 123.7 ± 0.5‰, $\delta^{18}O$ 16.24 ± 0.15 ‰, 1C: $\delta^{2}H$ 154 ± 0.5‰, $\delta^{18}O$ 19.49 ± 0.15‰. The laser machine can provide accurate results with an accuracy of approximately 1 ‰ for $\delta^{2}H$ and 0.2 ‰ for $\delta^{18}O$ in liquid water samples of up to at least 1000 mg/L dissolved salt concentration. The d-excess data in table 3 were calculated using equation 2 of the JMWL:

$\delta^{2}H = 6.7\ \delta^{18}O + 10$ (‰) *(Equation 2)*

d-excess = $\delta^{2}H - 6.7\ \delta^{18}O$ (*Equation 3)*

3.2.3 Radionuclide analysis

The analysis of the radionuclides of interest (U, Th, Ra, and Pb) was done at the South African Nuclear Energy Corporation (NECSA). The water samples were first filtered then acidified and then analysed using the alpha spectrometry and the liquid scintillation counter. Before counting, the samples were sealed for about 30 days to allow the radionuclides to reach circular equilibrium. Water samples are generally expected to have very low concentrations and using detectors with high sensitivity such as the LSC and other gas proportional counters, is important. Gas proportional counters have very high sensitivity since they used photomultiplier tubes to enhance even the smallest concentrations recorded by the detector (EMSL, 1980). It is this quality of gas proportional counters that is useful for the detection of radiation in very

small quantities. Gamma spectrophotometers may be used for low energy radiation detection measurements, while alpha spectrometry may be used for high energy measurements (Kaplan *et al*., 1995). Like the LSC, alpha spectrometry is sensitive and can measure both α- and β-emitters (Kaplan *et al.*, 1995).

The radionuclide analysis yielded activity concentration presented as spatial distribution maps in Figures 8-18. The effective doses were calculated using these activity concentrations. The effective dose serves as an estimate of the damage linked with exposure to ionising radiation and is used for radiation protection purposes (Pintilie-Nicolov *et al.*, 2021). Effective dose accounts for all the tissues and/or organs susceptible to ionising radiation by inhalation or ingestion (Clement *et al.*, 2010). The effective dose coefficients from the ICRP publication 119 (Clement *et al.*, 2010) were used to calculate the effective dose. The ICRP (Clement *et al.*, 2010) calculates the effective dose as follows:

$$E = eA \qquad \textit{(Equation 4)}$$

where:

E = effective dose (Sv/L)

e = effective dose coefficient (Sv/Bq)

A = activity concentration (Bq/L)

Chapter 4: Results and Discussion

4.1 Physico-chemical parameters

Physicochemical parameters are a direct indicator of any changes which may occur in the water quality. From Table 1 the range of the measured pH values lies within the allowed range of 6.5-8.5 (DWAF, 1996; WHO, 2011). The TDS values directly reflect the concentration of dissolved solids in the water. Since TDS is directly proportional to EC, the EC value increases as the TDS concentration increases. The maximum temperature (24.7°C), EC (1208 µS/cm) and TDS (775 mg/L) of sample ZN-29 may be a direct result of the land use in the area. The sample ZN-29 is located opposite a crop farm (approximately 500 m away) and about 300 m from a wetland. The high content of solids/salts could be leached from the excess fertilizers used on the crop farm. There is an active mine located approximately 5 km away from the borehole where sample ZN-29 was collected, and this could be another reason for the high EC and TDS. The local mineralogy surrounding this borehole could be another reason for the elevated EC and TDS, the sample ZN-29 lies in the Pretoria and Silverton Groups consisting of shale, quartzite, conglomerates, basalts, and some minor limestone. The borehole sample ZN-29 has a relatively short residence time suggesting that the elevated EC and TDS could be due to the highly enriched recharging water and not leached out from the geology. Sample ZN-35 reported the lowest temperature of 19.5 °C and this could be an indication of deep circulating waters. Sample ZN-27 reported the lowest EC (310µS/cm) and TDS (177.2 mg/L) values. Sample ZN-27 is a spring sample with a short residence time which could be used to explain the low EC and TDS concentrations. This reduces the contact time/interaction between the water and the surrounding geological rocks (Abiye, 2011; Leketa *et al.*, 2019).

Table 1: *Physical and chemical parameters for six groundwater samples within the West Rand.*

Sample ID	Source	Temperature (°C)	EC (µS/cm)	TDS (mg/L)	pH
ZN14	Borehole	19.5	832	535	6.6
ZN29	Borehole	24.7	1208	775	6.7
ZN33	Borehole	21.5	302	206	6.9
ZN35	Borehole	19.7	960	616	6.7
ZN40	Borehole	22.1	932	591	7.0
ZN27	Spring	20.8	310	177	7.5
Min.		**19.5**	**310**	**177**	**6.6**
Max.		**24.7**	**1208**	**775**	**7.5**
Mean		**21.4**	**707**	**452**	**7.0**

4.2 Activity concentration and effective dose of radionuclides

4.2.1 Uranium

The ^{234}U measured in the samples ranged between 15.3 and 210 mBq/L with an average of 65.34 mBq/L. Uranium-234 was recorded throughout the study area with very low activity concentrations with only one borehole sample ZN-14 (210 mBq/L) exhibiting very high activity concentration (Figure 8). ZN-14 was sampled from the Krugersdorp town and the high activity concentration may be due to the geology of the area as there are no mines visible in the area. Sample ZN-14 lies in the Swazi geology (basement) which comprises granitic gneiss rocks. Sample ZN-31 from the Fochville town is the second highest with a moderate activity concentration and this could be due to the Silverton shale in the area. According to Cowart and Burnett (1994) uranium is commonly found in granitic rocks as well as in shales and this could be used to explain the activity concentrations reported. There are visible mine tailings dams in the vicinity of the sampling point, and these could be the reason for the reported values. The activity concentrations of ^{234}U do, however, fall within the desired activity concentration of 30 µg/L (WHO, 2011) and 3.6 Bq/L (Forestry, 1996) in drinking water.

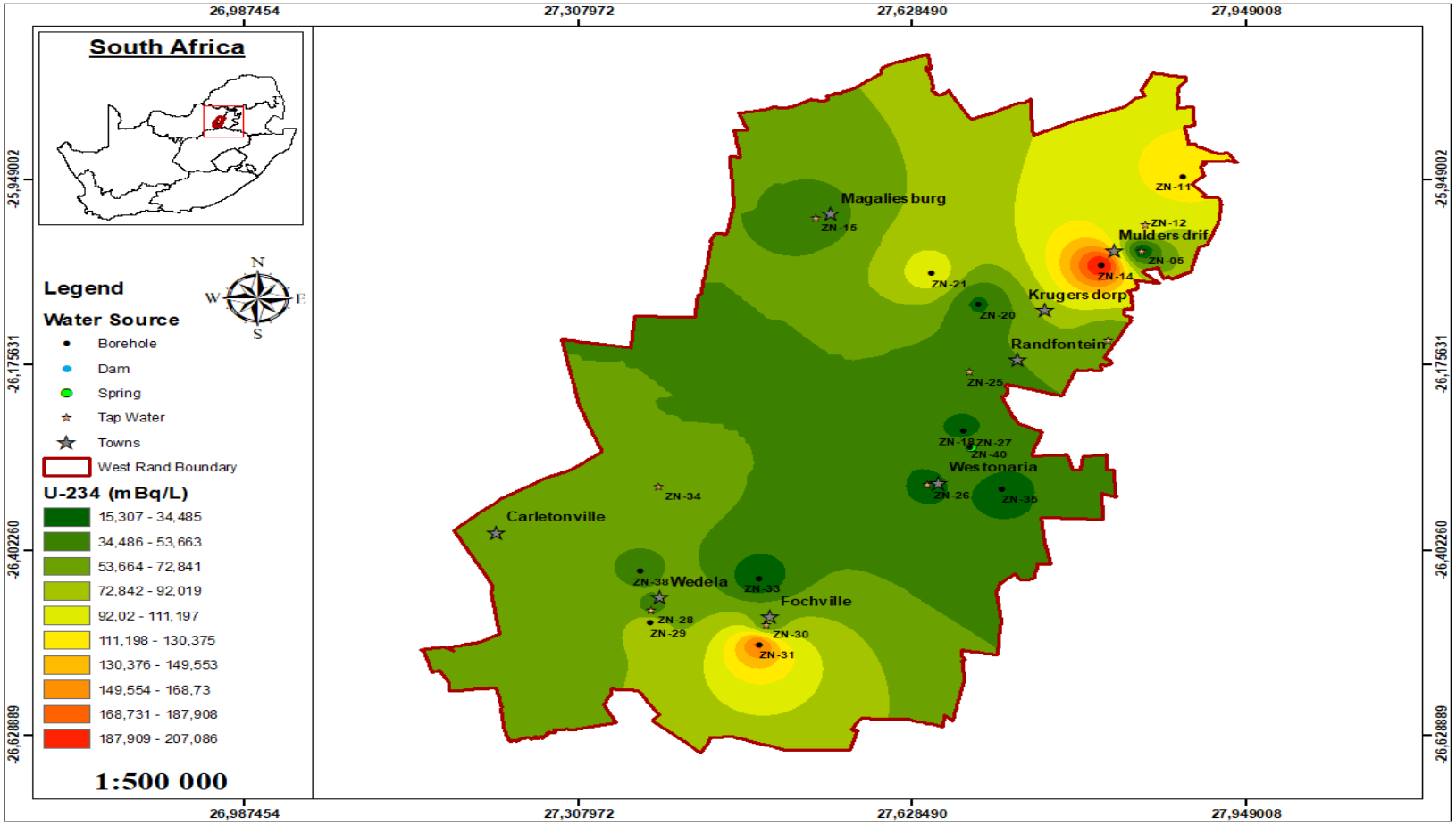

Figure 8: *A map illustrating the distribution of* ^{234}U *within the West Rand.*

According to Figure 9, ZN-11 (2.85 mBq/L) and ZN-14 (2.73 mBq/L) show the highest activity concentration of ^{235}U. The two samples with the highest activity concentration are boreholes samples and this could be attributed to the geology of the area. Sample ZN- 11 lies on the Halfway House granite which comprises of granodiorite. Cowart and Burnett (1994) suggest that uranium is highly abundant in granitic rocks. The quantity of uranium may vary in different granitic rocks as various fractionation processes take place (Cowart and Burnett, 1994; Faanu *et al.*, 2011). Since the mean pH of the groundwater samples is neutral, it could be proposed that the mobility of ^{235}U has been reduced as it forms salts under neutral conditions (Hamutoko *et al.*, 2014). Samples ZN-27 (spring) located in Westonaria and ZN-15 (tap water) from Magaliesburg both have moderate activity concentrations, and this is anomalous to the surrounding towns which show very low activity concentrations of ^{235}U. The ^{235}U activity concentrations are generally low and fall well under the allowed WHO activity concentration guidelines for drinking water. These low activity concentrations could be attributed to the relatively low natural abundance of ^{235}U.

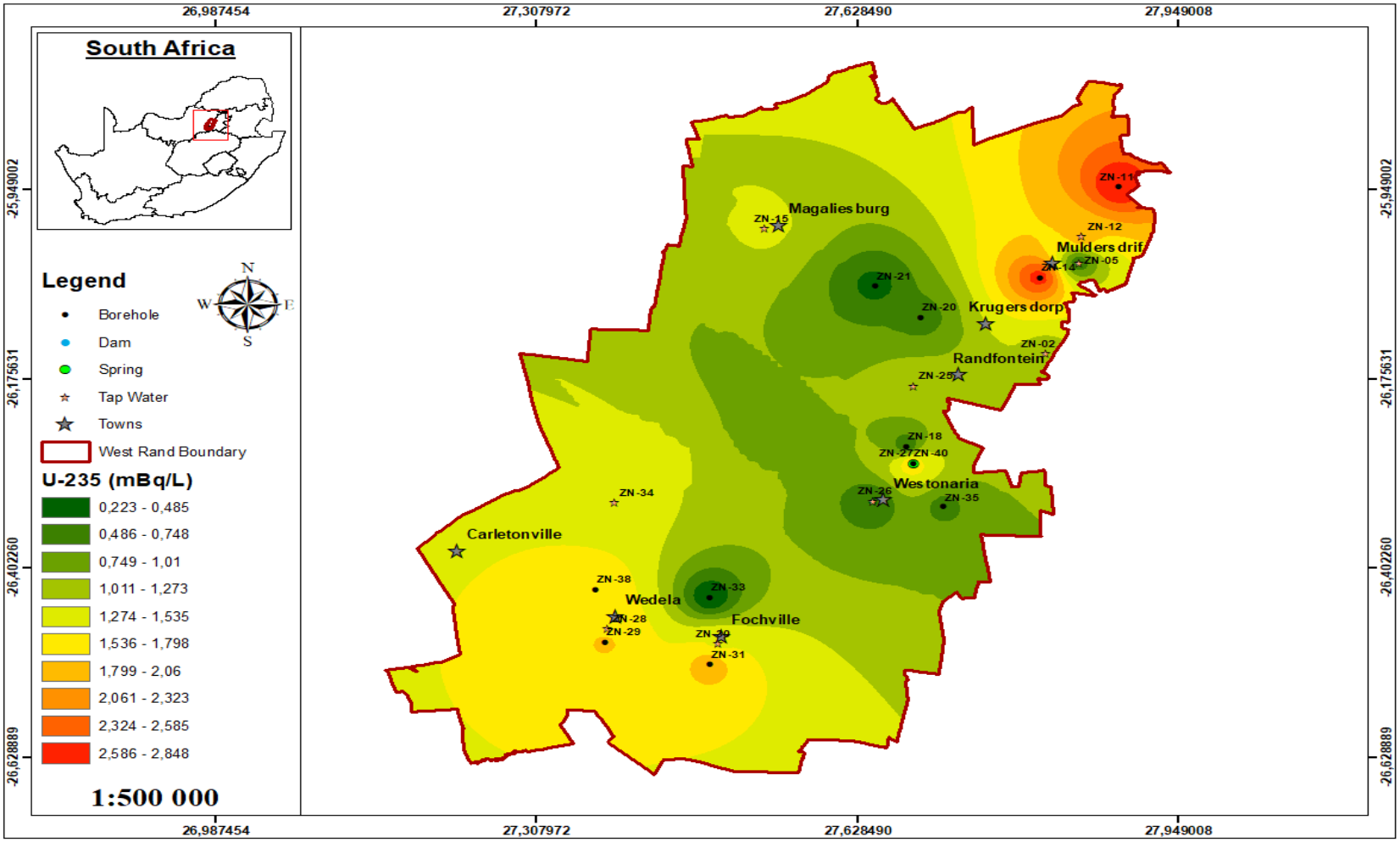

Figure 9: *A map illustrating the ^{235}U distribution within the West Rand.*

The distribution map in figure 10 shows a moderate to low distribution of ^{238}U ranging between 4.73 and 62.0 mBq/L. The borehole samples ZN-11 (62.0 mBq/L) and ZN-14 (59.3 mBq/L) which were collected in Lanseria and Krugersdorp, respectively, appear to have the highest activity concentrations of ^{238}U. The sample ZN-11's high activity concentration is due to its location on an inter-angular and fractured aquifer with yields of 0.5-2 L/s on the Halfway House granite. Granites are most likely to have fractures and fissures along which water can flow. Granites are known to house uranium and thorium thus the high activity concentrations could mean that the uranium was leached out of the bedrock and mobilized into the water (Kim and Osseo-Asare, 2012). This aquifer has a series of rivers running it. The rivers could be the means of recharge for this aquifer and may also be responsible for the radionuclide contamination. The possible source of this contamination carried by the rivers could be AMD or spillages upstream of these rivers from the local mines especially in the Krugersdorp area or from fertilizers in the Lanseria region. Studies conducted by Lapworth et al. (2021) suggest that fertilizers contain nitrates which have the potential to mobilise uranium. Sample ZN-33 reported the lowest activity, and this could be attributed to the various conditions in redox potential, pH and the source rock from where the sample was collected (Lapworth *et al.*, 2021). Lapworth et al. (2021) explain that uranium is stable in oxidising environments with neutral pH with no microbial activity. The activity concentration of ^{238}U lies well below the allowed WHO limit (30 μg/L) for drinking water.

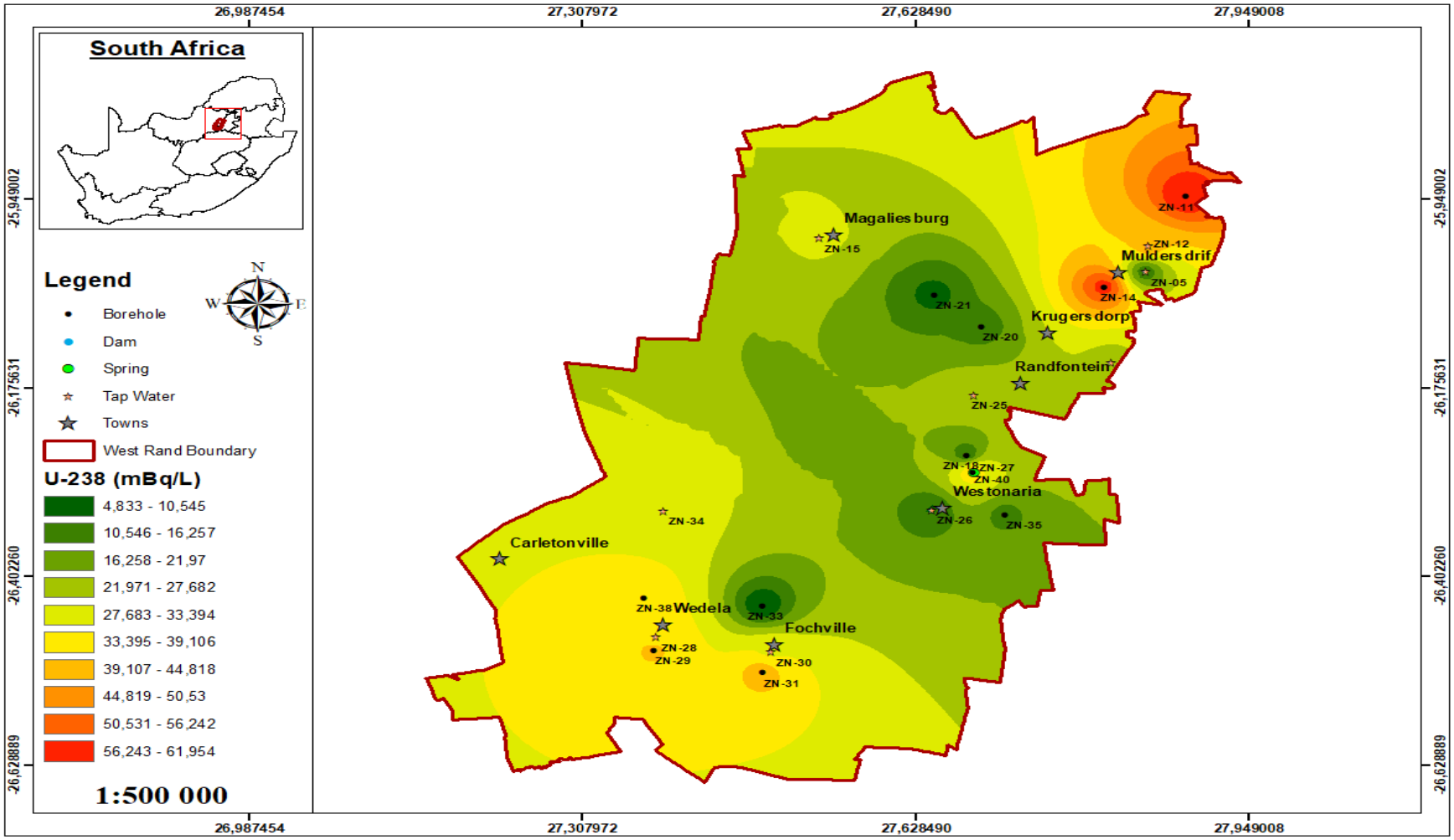

Figure 10: *A map showing the distribution of* ^{238}U *within the West Rand.*

4.2.2 Thorium

According to figure 11, ^{227}Th has a low to moderate distribution with activity concentrations ranging from 2.28 to 50.5 mBq/L. Sample ZN-34 (municipal tap water) is anomalous and has the highest activity concentration of 50.5 mBq/L. The source of the municipally supplied water is the Vaal dam, it could be attributed to the high activity concentration reported by sample ZN-34. Tap water supplied by the municipality is usually sourced from local dams and is pre-treated with the aim of removing all harmful substances (Alexander *et al.*, 1954). Since open bodies of water such as the Vaal dam are treated and purified to supply water to residential areas, fall-out atmospheric radionuclides may easily be introduced to the system in such ways (Alexander *et al.*, 1954). Samples ZN-15 (34.7 mBq/L), ZN-30 (38.2 mBq/L) and ZN-35 (37.7 mBq/L) show moderate activity concentrations. Thorium does not readily dissolve in soil or groundwater and this could be the explanation for the low Th activity concentrations within the study area (Rosner *et al*., 2001). The half-life of ^{227}Th is 18.69 days which is short when considering the sealing of samples before analysis, yet the measured activity concentrations were not lower than the background of the detector. This suggests that the sample had a significantly high activity concentration of ^{227}Th, and this could be attributed to the Th-rich shale rocks which are known to be the common hosts for Th (Beers, 1945; Cowart and Burnett, 1994).

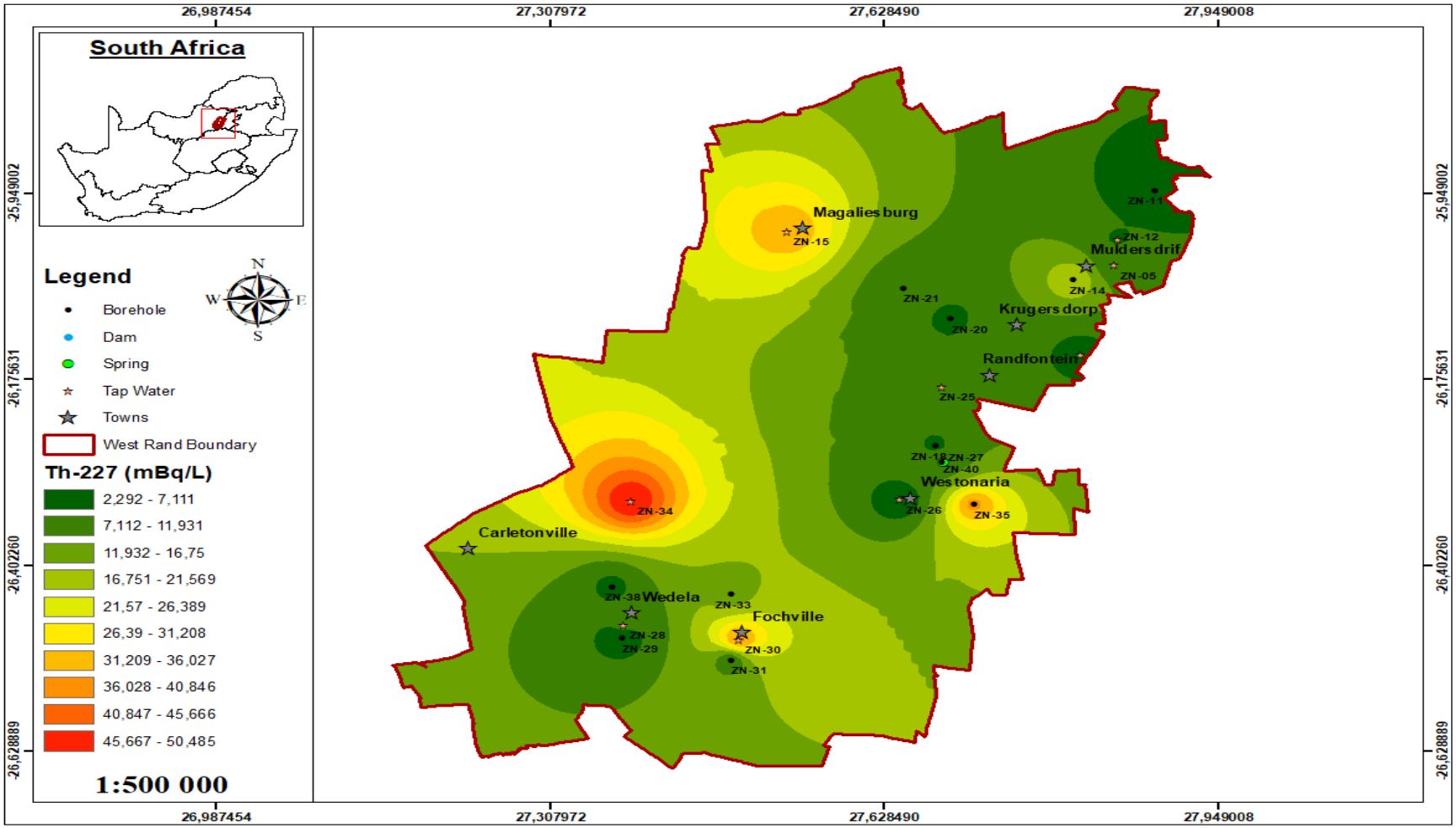

Figure 11: *A map illustrating the* ^{227} *Th distribution within the West Rand.*

Based on Figure 12, the general activity concentration of ^{228}Th ranges from moderate to low with only three samples having very high activity concentrations (4.73 – 33 mBq/L). Sample ZN-26 (33.0 mBq/L) collected from Westonaria shows the highest activity concentration, followed by borehole samples ZN-18 (31.6 mBq/L) and ZN-38 (31 mBq/L), respectively. Sample ZN-38's high activity concentration could be due to the Pretoria Group rocks that form part of the Transvaal Supergroup where the sample was collected. The Pretoria group consists of conglomerate and carbonate rocks which are well known hosts of Th (Cowart and Burnett, 1994). The sample ZN-36 (15.9 mBq/L) from the Vaal dam has a concentration activity lower than that of ZN-26 which suggests that there may be an external source of radiation along the pipelines where the water is supplied to households. Studies done by Alexander *et al.*, (1954) suggest that municipal water supplies may also be contaminated with radionuclides by means of accidental spills from nuclear reactors and nuclear fall-out from atmospheric radionuclides. Tap water supplied by the municipality is usually sourced from local dams and is pre-treated with the aim of removing all harmful substances (Alexander *et al.*, 1954). The low activity concentrations reported from the Vaal dam (ZN-36) suggest that there is very little contamination due to radiation fallout. The samples in Magaliesburg, Muldersdrift, Krugersdorp and Randfontein have very low activity concentrations which are expected since sample ZN-36 which is the source, has a low activity concentration for ^{228}Th. The mean ^{228}Th activity concentration is within the allowed DWAF drinking water guideline of 0.228 Bq/L.

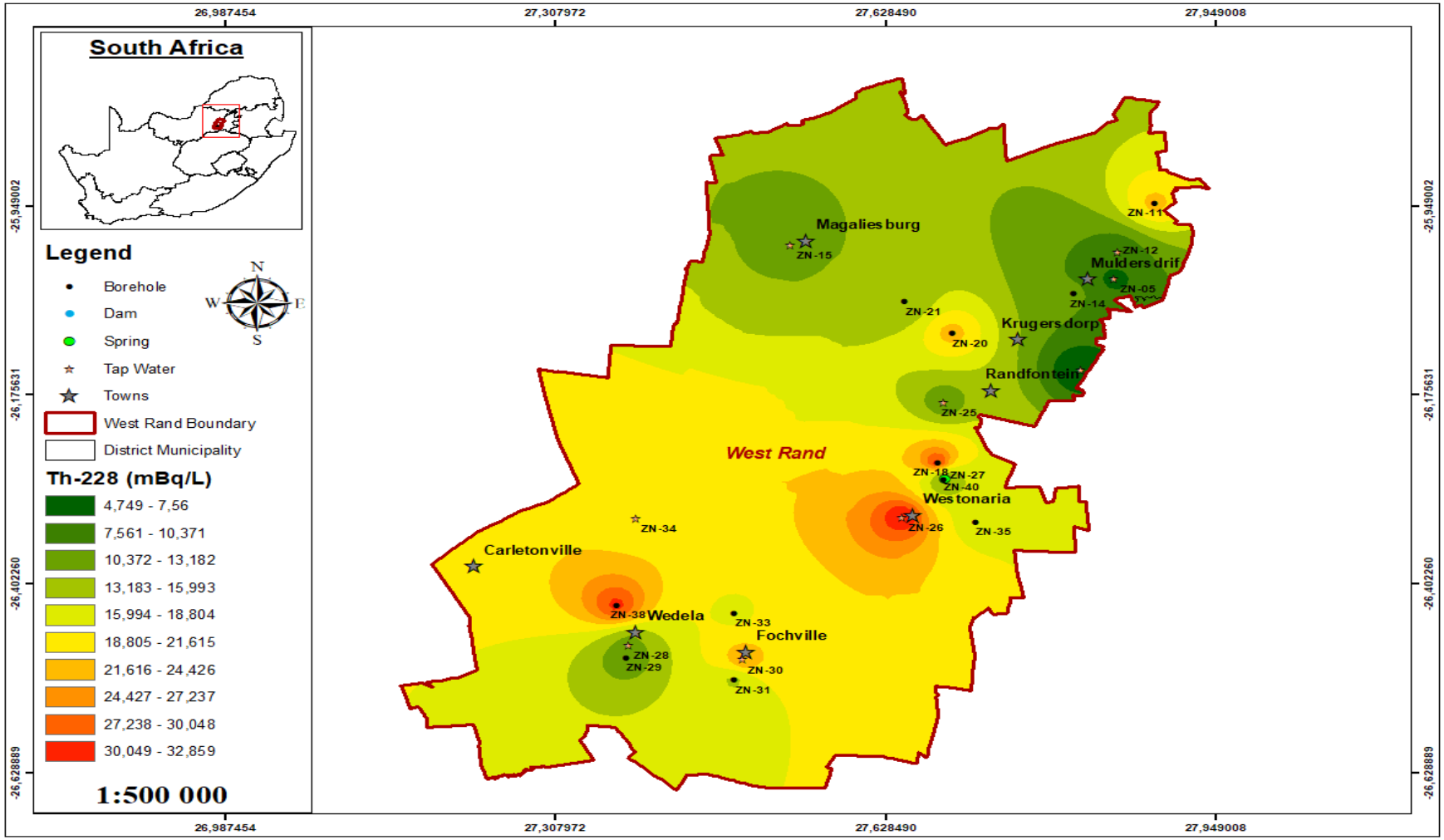

Figure 12: *A map illustrating the* ^{228} *Th distribution within the West Rand.*

Figure 13 shows a distinct ^{230}Th pattern where neighbouring samples have varying activity concentrations from each other. The general pattern suggests that the activity concentrations range from very low (18 mBq/L) to very high (86.4 mBq/L) from samples ZN-34 and ZN-40, respectively. The municipally supplied tap water samples ZN-34 (18 mBq/L) and ZN-30 (28 mBq/L) have very low activity concentrations and this could be attributed to the fact that is formed by the disintegration of ^{234}U ($2.55x10^5$ years). Samples ZN-40 (86.4 mBq/L), ZN-29 (79.5 mBq/L), ZN-33 (78.9 mBq/L), ZN-21(70.2 mBq/L) and ZN-14 (72.6 mBq/L) show very high activity concentrations. The elevated activity concentrations could be attributed to the geology of the area which contains Th-rich shales (Beers, 1945). According to Beers (1945) and Cowart and Burnett (1994) the rocks in which samples were collected determine the activity concentrations reported. Shales and granitic rocks are rich in U and Th (Cowart and Burnett, 1994). The ^{230}Th activity concentrations lie within the allowed DWAF drinking water guideline with the activity level of 0.228 Bq/L.

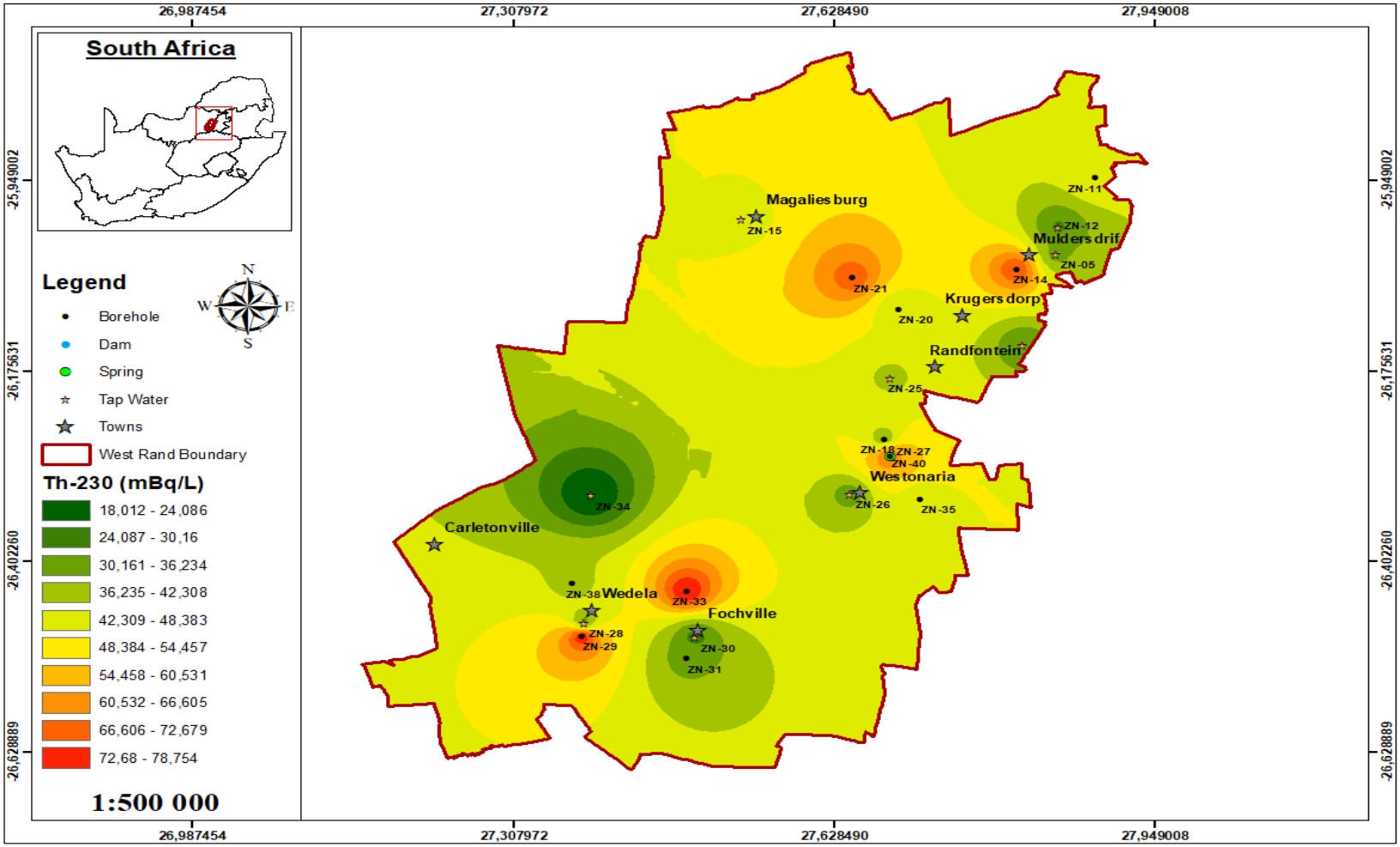

Figure 13: *A map illustrating the ^{230} Th distribution within the West Rand.*

^{232}Th is abundantly and readily found in nature. The West Rand region generally has a moderate to low activity concentration. Based on Figure 14 samples ZN-30 (23.5 mBq/L), ZN-21 (21.6 mBq/L), and ZN-31 (21.7 mBq/L) have the highest activity concentration of ^{232}Th. Samples ZN-30 and ZN-31 are located close to each other and share the same geology (Silverton Shale) which is Th-rich. A study conducted by Cowart and Burnett (1994) suggests that thorium is most likely to be hosted in shales and granitic rocks. Sample ZN-21 lies in the Malmani Subgroup which also contains carbonaceous shale. The sample with the lowest activity concentration is ZN-20 and is in Krugersdorp approximately 5km away from a prominent mine tailings dump. The visible mine tailings dumps which could be well shielded or may contain very few radionuclides. The low activity concentrations suggest that Th may have decayed over time. The overall activity concentration for all the samples lies within the allowed WHO and DWAF drinking water guidelines limit.

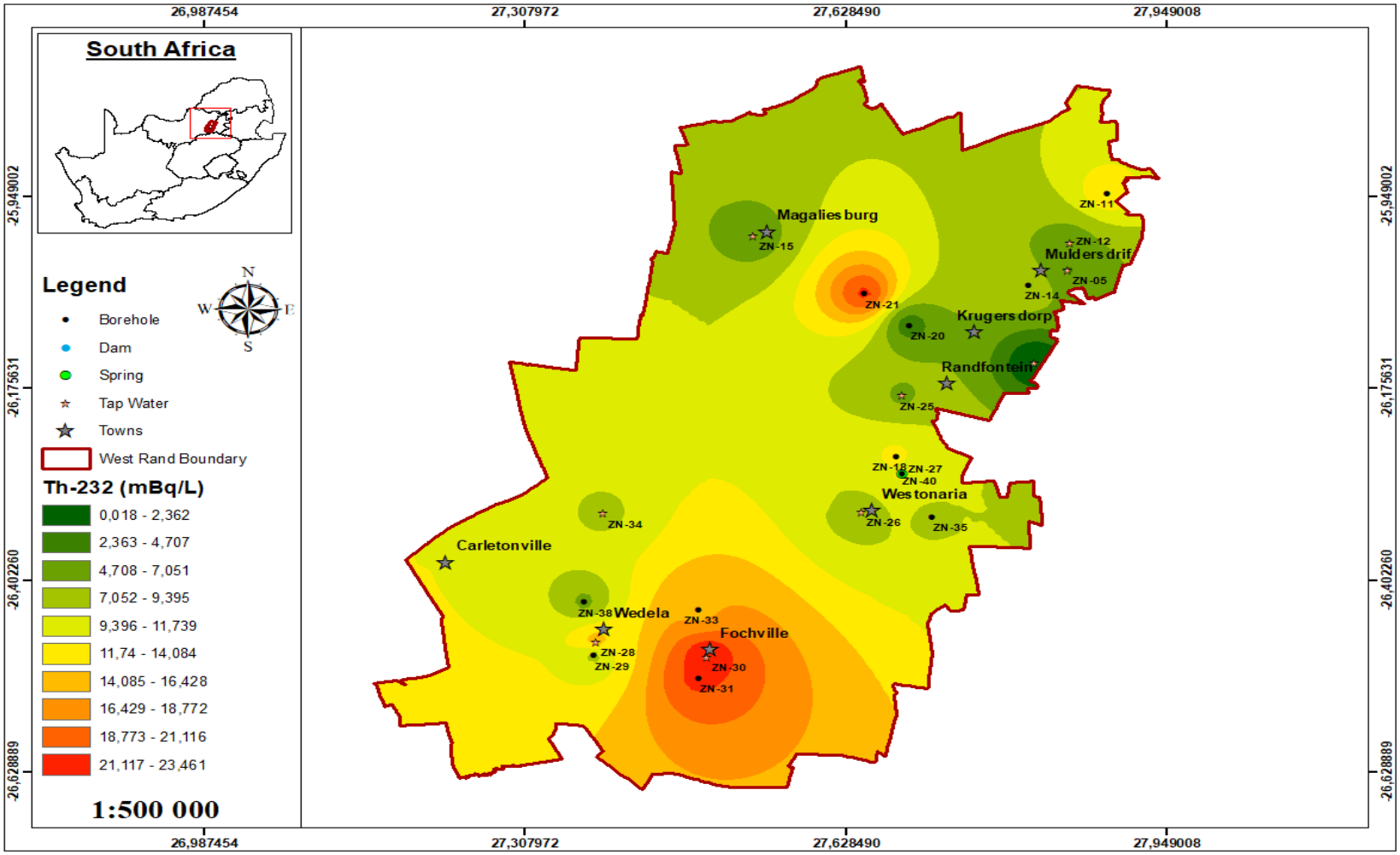

Figure 14: *A map illustrating the* ^{232} *Th distribution within the West Rand.*

4.2.3 Radium

^{223}Ra and ^{224}Ra have very short half-lives of 11.4 days and 3.6 days, respectively. These half-lives are extremely short since the samples need to be sealed for at least 30 days for the radionuclides to reach circular equilibrium before any analyses are done. The samples were only analysed after months hence the measured values reflect very low activity concentrations.

^{226}Ra is not readily found in nature and forms from the decay of ^{230}Th (IAEA, 2011). According to Figure 14, ZN-11 and ZN-21 have the highest ^{226}Ra activity concentrations of 19.5 mBq/L and 13.5 mBq/L. The presence of ^{226}Ra in the study area indicates that there was ^{230}Th within the study area which has now decayed, while its absence would suggest the opposite. Samples ZN-36, ZN-34 and ZN-33 show moderate activity concentrations and the remaining samples show very low activity concentrations. Based on Figure 15, samples ZN-02, ZN-15, ZN-18, ZN-25, ZN-26, and ZN-28 all reported negative activity concentrations which indicate that the background activity of the detector is higher than that of the samples. The negative activity concentrations show that ^{226}Ra contributes very little radiation to the study area environment and lies within the allowed Department of Water Affairs and Forestry drinking water benchmark of 0.42 mBq/L.

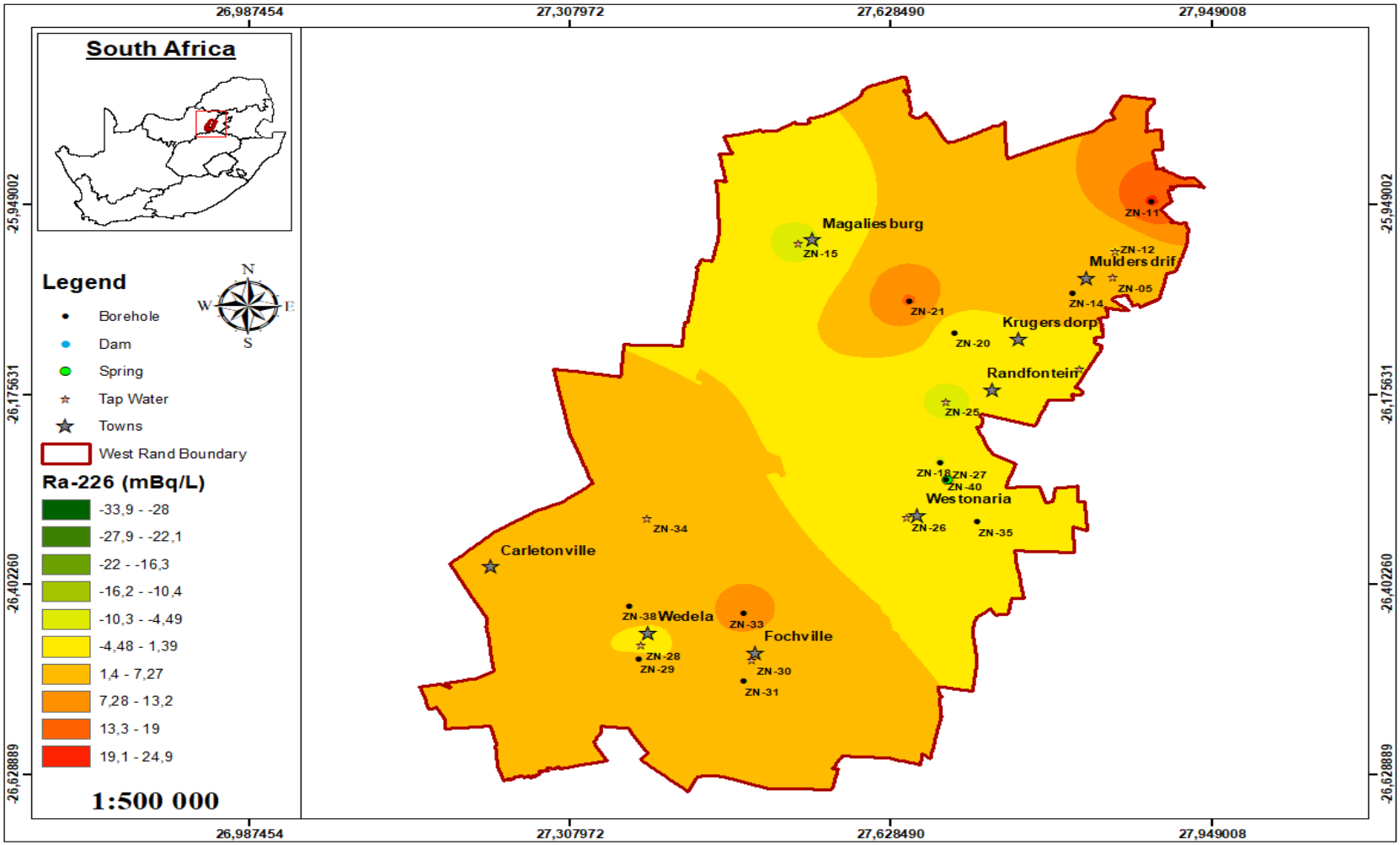

***Figure 15**: A map illustrating the ^{226}Ra distribution within the West Rand.*

4.2.4 Lead

This study focused on ^{210}Pb which reported activity concentrations that ranged from 1.2 to 135 mBq/L with an average of 20.35 mBq/L. Based on Figure 16, the general distribution of ^{210}Pb is generally low with one sample ZN-38 having a very high activity concentration of 135 mBq/L. Three other samples ZN-29 (107 mBq/L), ZN-21 (61.5 mBq/L) and ZN-11 (58.1 mBq/L) also reported higher activity concentrations. All these samples having significantly high activity concentrations are the borehole samples which may be a direct result of the geology since they are relatively distant from each other or from taps connected to the borehole system. Pb is usually present in small concentrations in tap water, and this is mainly from household plumbing systems (WHO, 2004). All these samples (ZN-38, ZN-29, ZN-21, ZN-11) come from various lithologies. Sample ZN-38 lies in the Pretoria Group, which is made up of shale, quartzite and breccias while sample ZN-29 lies on the border between the Pretoria Group and the Silverton Group consisting of shale, minor limestones, basalt, and tuff. According to Ram *et al.* (2021), Pb is usually found in igneous rocks such as granites where all these samples appear. Samples ZN-38 and ZN-29 are, however, linked by the aquifer containing shale, and this could be the cause of the elevated ^{210}Pb activity concentrations reported. Samples ZN-11 and ZN-21 may be linked by the rivers cutting through the areas where the samples were collected. The samples are all within the WHO (2011) drinking water guidelines of 0.2 Bq/L.

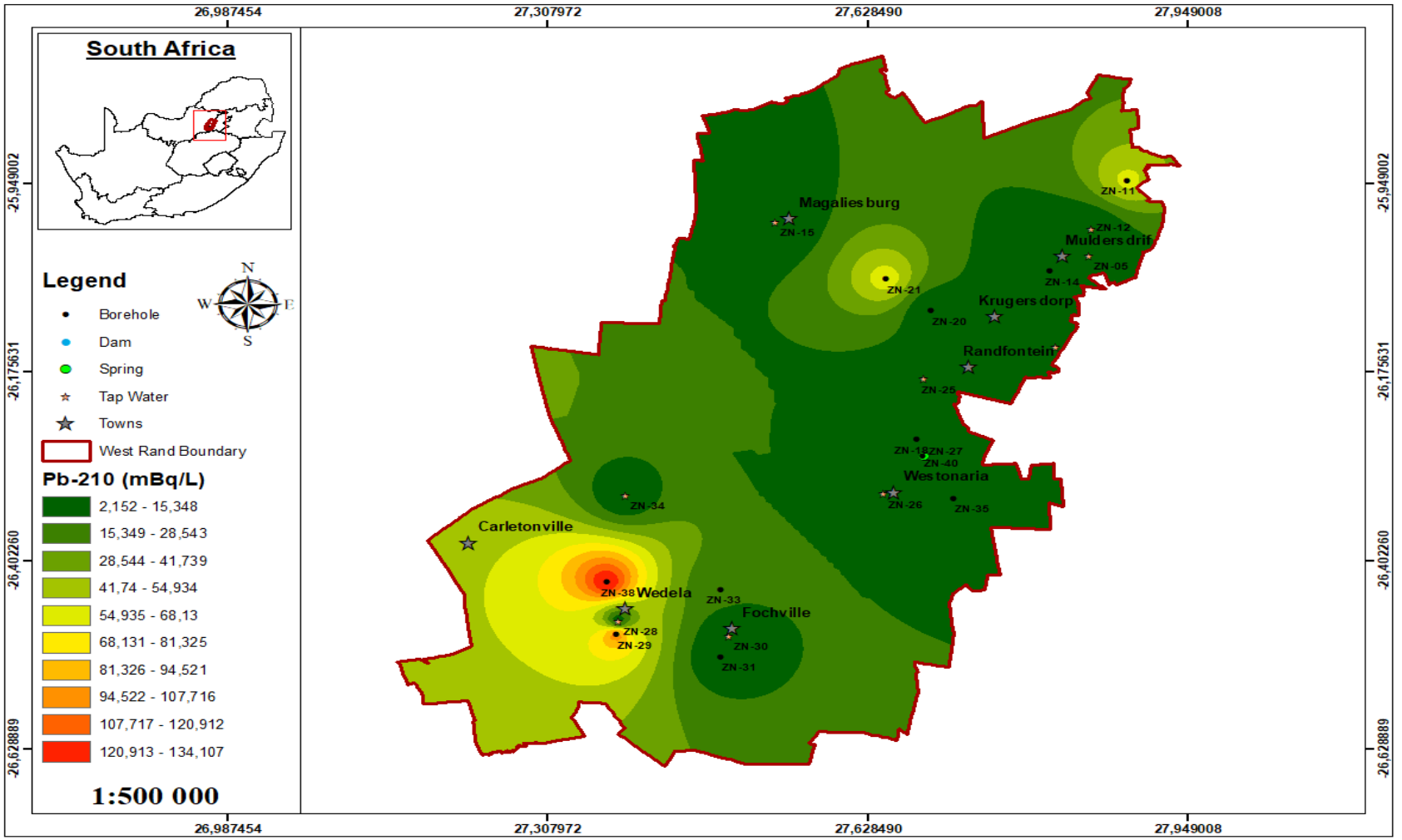

Figure 16: *A map illustrating the ^{210}Pb distribution within the West Rand.*

4.2.5 Gross alpha

The spatial distribution map in Figure 17 shows the general distribution of gross alpha activities within the study area. The gross alpha activities range from -16 to 341 mBq/L. The two towns which exhibit very high gross alpha activities are Westonaria with sample ZN-11 (341 mBq/L) and Lanseria with sample ZN-35 (321 mBq/L) (located just above Muldersdrift). Most of the radionuclides assessed in this study are long-lived alpha emitters and will thus emit alpha particles/ decay at a relatively slow rate. Sample ZN-02 reported the lowest gross-α which suggests that the sample may contain very few alpha emitters as compared to sample ZN-11 which reported the highest gross-α activities.

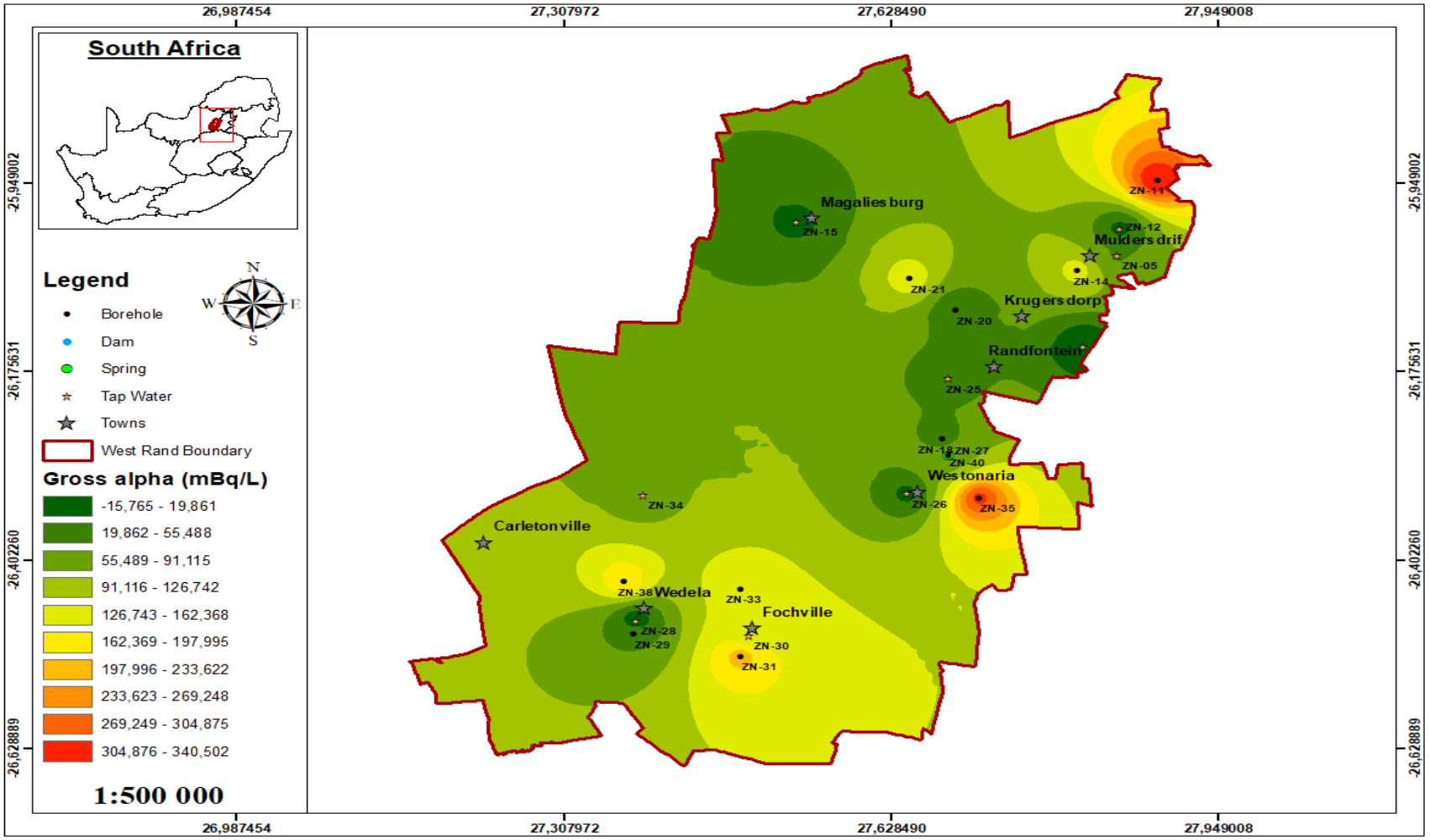

Figure 17: *A spatial distribution map illustrating the gross-α activity distribution in the study area.*

4.2.6 Gross beta

The spatial distribution map in Figure 18 generally shows very little gross beta activity across the study area with one sample ZN-30 having the highest activity concentration of 13500 mBq/L. Samples ZN-25 (2380 mBq/L), ZN-35 (673 mBq/L), ZN-31(604 mBq/L) and ZN-11 (502 mBq/L) show moderate beta activities. Sample ZN-25 is a municipally supplied tap water sample while ZN-11 was sampled from a borehole. The elevated gross-β activity concentration reported by sample ZN-11 could be due to Pb- rich shales that make up the geology of the area. Lead is a beta emitter (Kaplan *et al.*, 1995) and could be the reason for the elevated activity concentration reported by sample ZN-11. The high gross-β activity concentrations in the municipal supplied tap water sample ZN-25 could be due to the corroded pipes/ infrastructure used to transport the water to households. Studies have shown that one of the ways in which Pb is introduced in water is through corroded pipes (DWAF, 1996). The DWAF (1996) further explains that water with low pH may exacerbate the corrosion of pipes, therefore, introducing Pb into water systems. Municipalities usually treat and purify water from local dams to supply to households (Alexander *et al.*, 1954). In the West Rand region, the municipality sources its water from the Vaal dam and this could be where the Pb contamination originates as the Vaal Dam is fed by many rivers. The sample with the lowest gross beta activity is ZN-29 (-1100 mBq/L). The negative activity concentration suggests that the gross-β activity concentration is lower than that of the background of the detector. The gross-β activity concentrations lie within the WHO drinking water guidelines of 1 Bq/L, with one sample ZN-30 being above the guidelines.

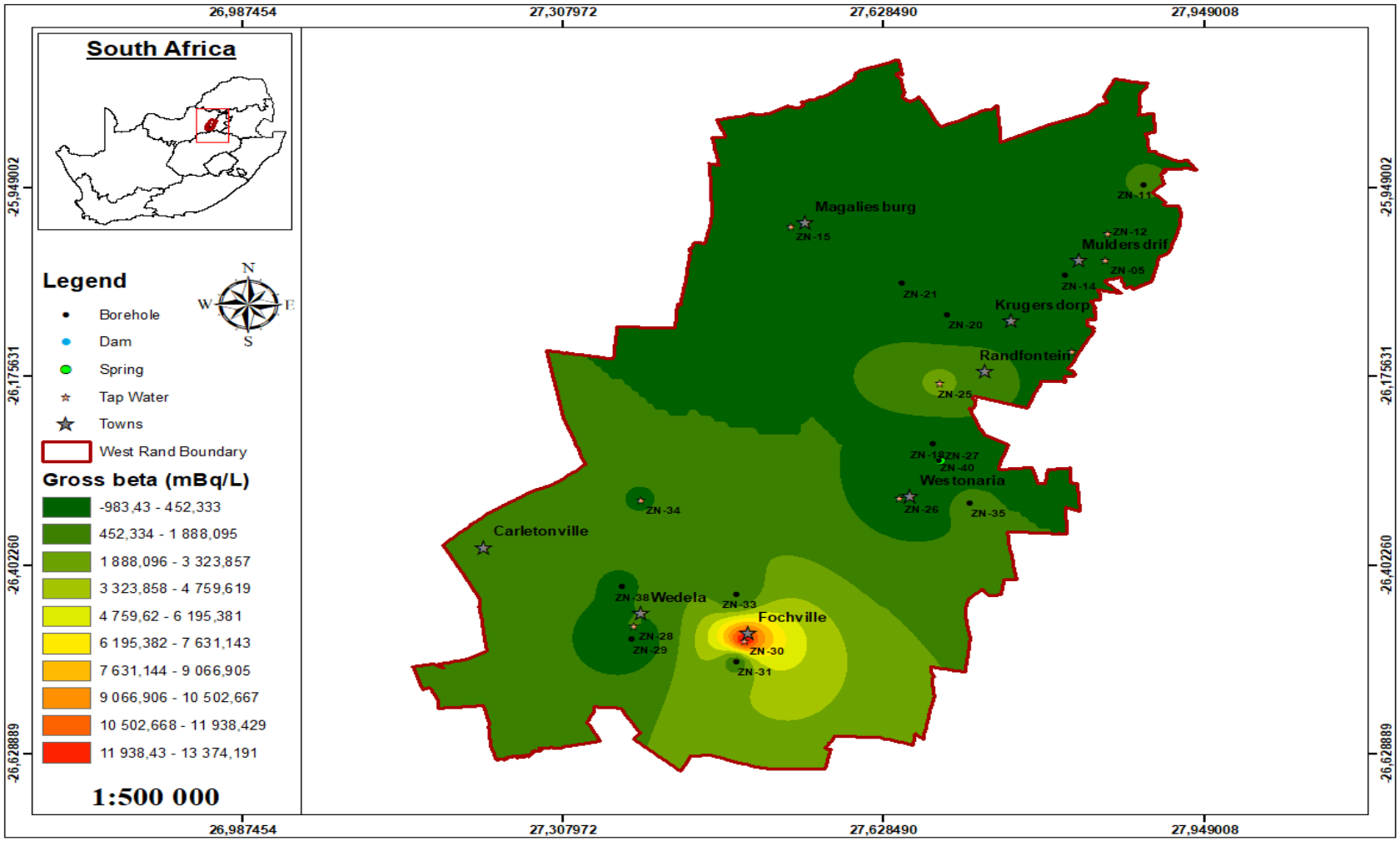

***Figure 18**: A spatial distribution map illustrating the gross beta activity distribution in the study area.*

Figure 19 shows a comparative histogram of the measured radionuclide activity concentrations against the recommended activity concentrations. Based on the chart, the measurements are significantly smaller than the recommended values. This could be due to the waiting time before analysis. The recommended waiting period is approximately thirty days and allows for the mother and daughter radionuclides to decay at the same rate (L'Annunziata, 2012). The samples were kept for longer than the recommended waiting time hence the low measured activity concentrations. It could also be inferred that the samples originally had significantly low activity concentrations despite the long waiting time before analysis.

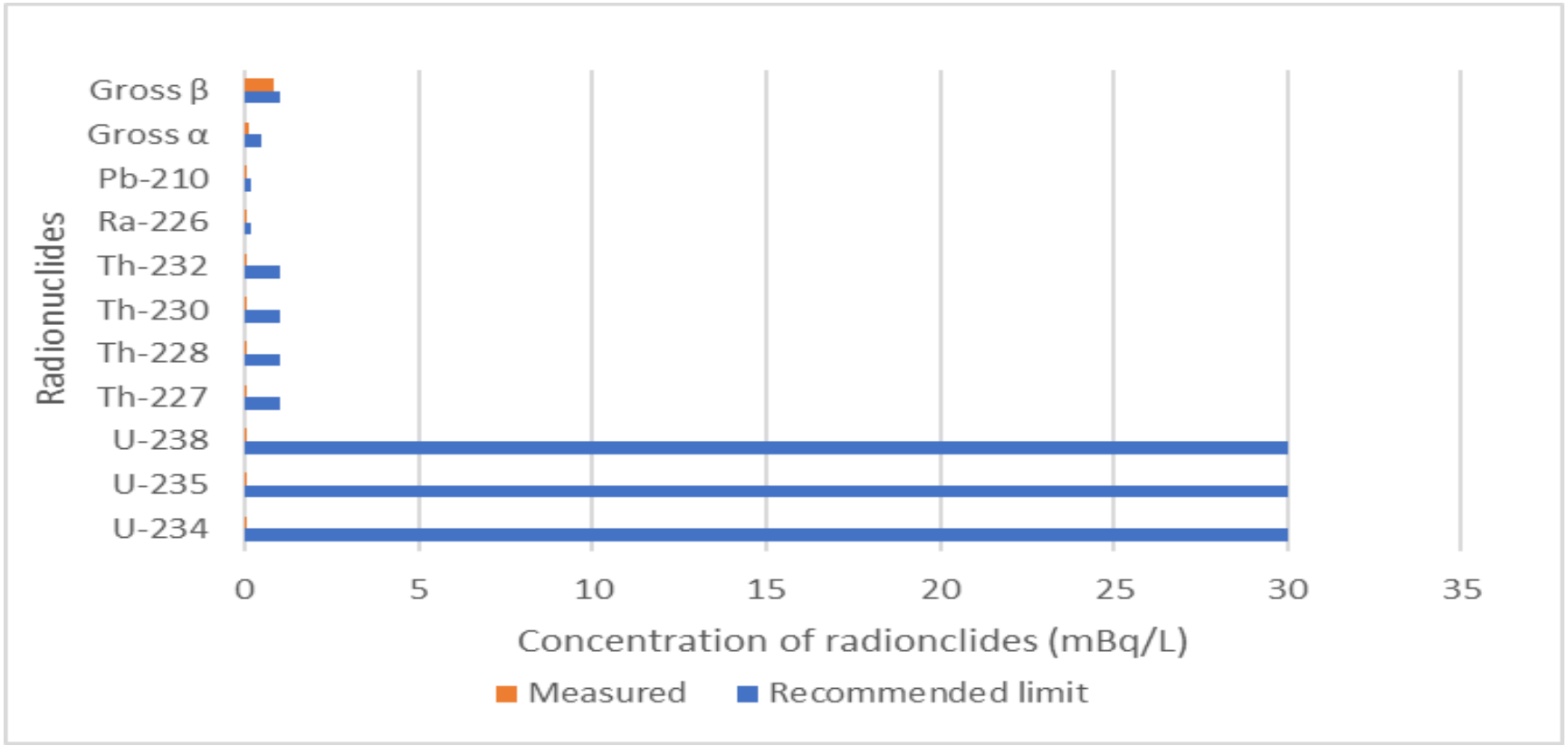

Figure 19: *A comparative plot showing the measured radionuclide activity concentrations versus the recommended activity concentrations.*

4.2.7 Effective dose

Effective dose is a criterion used to calculate the risks associated with radiation exposure and accounts for all the organs which may be affected by the absorbed radiation (Kaplan *et al*., 1995). NORMs are responsible for approximately 65% of the radiation humans and animals are exposed to (UNSCEAR, 2000). The effective dose from ingestion is an important parameter that can be used during the establishment of radiation protection policies (UNSCEAR, 2000; WHO, 2011). Table 2 shows the effective dose from ingestion for each radionuclide of interest in this study. The effective dose measured for ^{234}U ranges between 9.41x10^{-13}(ZN-05) to 1.03x10^{-8} (ZN-14) Sv/L with an average of 3.16x10^{-09} Sv/L. The highest effective dose was from a borehole sample located in Krugersdorp and the lowest effective dose was measured from a tap water sample from Muldersdrift. It is expected that a municipally supplied tap water sample reports low effective doses as it has been treated and purified for human consumption. For ^{235}U, the range of the effective dose due to ingestion is from 1.02 x10^{-11} Sv/L (ZN-33) to 1.34 x10^{-10} Sv/L (ZN-11) with an average of 6.16x10^{-11} Sv/L. Both the samples ZN-33 and ZN-11 were collected from boreholes. The high effective dose in sample ZN-11 could be due to its location as well as the local geology. ^{238}U is the most abundant isotope of uranium with its effective dose ranging between 2.13x10^{-10} Sv/L and 2.67x10^{-6} Sv/L from samples ZN-33 and ZN-14 respectively. Both these samples are borehole samples. The sample ZN-14 with the highest effective dose is comprised of quarzitic and gneissic geology.

The highest effective dose for ^{227}Th was sample ZN-34 (4.44x10^{-10} Sv/L) and sample ZN-11 (2.13x10^{-10} Sv/L) reported the lowest with an average of 1.25x10^{-10} Sv/L. The effective dose of ^{228}Th ranges between 3.41x10^{-10} Sv/L and 1.64x10^{-6} Sv/L with an average effective dose of 7.41x10^{-08} Sv/L. Sample ZN-11 is a borehole sample that reported the highest effective dose. 230Th and 232Th reported effective doses that ranged from 3.78x10^{-9} Sv/L to 1.81x10^{-8} Sv/L (ave. 9.79x10^{-09} Sv/L) and <MDA to 5.41x10^{-9} (ave. 2.54x10^{-09} Sv/L) respectively. Thorium is characterized by its low solubility in water (Kaplan et al., 1995) and this could be the reason for the low effective doses reported for thorium isotopes. ^{226}Ra can be associated with effective doses ranging from -1.79x10^{-9} Sv/L (ZN-25) to 5.46x10^{-9} Sv/L (ZN-11) with an average of 6.43x10^{-10} Sv/L. The samples which reported negative effective doses were a direct result of the low activity concentrations reported. These negative results show that the activity concentrations of radium were significantly smaller than the background activity of the

detector. DWAF (1996) suggests that the mobility of thorium and radium is a direct consequence of the insoluble sulphate and phosphate salts they form.

Lead is known for its radiotoxicity and this quality requires that it be carefully monitored. The effective dose of ^{210}Pb ranged between $8.28x10^{-10}$ Sv (ZN-28) and $9.32x10^{-8}$ Sv/L (ZN-38) with an average of $1.40x10^{-08}$ Sv/L. The sample with the highest effective dose is a borehole sample, while the sample with the lowest effective dose is a tap water sample. The high effective dose could be a result of the geology of where the sample was collected. Most of the samples with the highest effective dose are borehole samples suggesting that the geology, as well as the aquifer systems of the areas where the samples were collected, has an impact on the radiation levels reported. All the samples of this study reported effective doses which are within the drinking water guidelines which state that the annual effective dose must be between 1 mSv/L and 3 mSv/yr (UNSCEAR, 2000; WHO, 2011). The South African domestic water guidelines state that the allowed effective dose limit is 1 mSv/L for civilians and up to 3 mSv/L for radiation workers (DWAF, 1996).

***Table 2**: A table illustrating the effective dose (e) from ingestion of the radionuclides of interest in Sv/L.*

Sample Id	e^{234}U (Sv/L)	e^{235}U (Sv/L)	e^{238}U (Sv/L)	e^{227}Th (Sv/L)	e^{228}Th (Sv/L)	e^{230}Th (Sv/L)	e^{232}Th (Sv/L)	e^{223}Ra (Sv/L)	e^{210}Pb (Sv/L)
ZN-02	$2.92x10^{-09}$	$5.50x10^{-11}$	$1.14x10^{-09}$	$4.46x10^{-11}$	$3.41x10^{-10}$	$6.51x10^{-09}$	<MDA	$1.20x10^{-10}$	$2.21x10^{-09}$
ZN-05	$9.41x10^{-13}$	$2.52x10^{-11}$	$5.27x10^{-10}$	$7.91x10^{-11}$	$4.83x10^{-10}$	$7.22 x10^{-09}$	$1.04x10^{-09}$	$1.60 x10^{-10}$	$2.01x10^{-09}$
ZN-11	$6.22x10^{-09}$	$1.34x10^{-10}$	$2.79x10^{-09}$	$2.01x10^{-11}$	$1.61x10^{-06}$	$1.01 x10^{-08}$	$3.06x10^{-09}$	$2.00 x10^{-10}$	$4.01x10^{-08}$
ZN-12	$5.49x10^{-09}$	$9.64x10^{-11}$	$2.01x10^{-09}$	$5.92x10^{-11}$	$6.25x10^{-10}$	$6.11 x10^{-09}$	$1.41x10^{-09}$	$2.30 x10^{-10}$	$1.46x10^{-09}$
ZN-14	$1.03x10^{-08}$	$1.28x10^{-10}$	$2.67x10^{-06}$	$1.87x10^{-10}$	$7.70x10^{-10}$	$1.52 x10^{-08}$	$2.09x10^{-09}$	$-1.30 x10^{-10}$	$2.31x10^{-09}$
ZN-15	$2.25x10^{-09}$	$6.20x10^{-11}$	$1.30x10^{-09}$	$3.05x10^{-10}$	$8.64x10^{-10}$	$9.83 x10^{-09}$	$1.39x10^{-09}$	$1.30 x10^{-09}$	$2.09x10^{-09}$
ZN-18	$1.20x10^{-09}$	$1.89x10^{-11}$	$3.93x10^{-07}$	$4.93x10^{-11}$	$2.28x10^{-09}$	$7.35 x10^{-09}$	$2.88x10^{-09}$	$1.50 x10^{-10}$	$4.28x10^{-09}$
ZN-20	$1.52x10^{-09}$	$2.88x10^{-11}$	$5.99x10^{-10}$	$5.46x10^{-11}$	$1.63x10^{-09}$	$9.24 x10^{-09}$	$8.28x10^{-10}$	$-8.40 x10^{-10}$	$2.28x10^{-09}$
ZN-21	$5.10x10^{-09}$	$1.80x10^{-11}$	$3.75x10^{-10}$	$8.54x10^{-11}$	$9.79x10^{-10}$	$1.47 x10^{-08}$	$4.97x10^{-09}$	$-2.00 x10^{-10}$	$4.24x10^{-08}$
ZN-25	$2.32x10^{-09}$	$5.64x10^{-11}$	$1.17x10^{-09}$	$6.84x10^{-11}$	$8.14x10^{-10}$	$8.55x10^{-09}$	$1.54x10^{-09}$	$5.70 x10^{-10}$	$7.59x10^{-09}$
ZN-26	$1.55x10^{-09}$	$2.16x10^{-11}$	$4.48x10^{-10}$	$2.31x10^{-11}$	$2.38x10^{-09}$	$6.93 x10^{-09}$	$1.78x10^{-09}$	$-2.60 x10^{-10}$	$8.14x10^{-09}$
ZN-27	$9.75x10^{-10}$	$4.30x10^{-11}$	$8.96x10^{-10}$	$8.98x10^{-11}$	$7.06x10^{-10}$	$9.22 x10^{-09}$	$6.23x10^{-10}$	$-7.10 x10^{-10}$	$1.18x10^{-09}$
ZN-28	$2.06x10^{-09}$	$7.94x10^{-11}$	$1.66x10^{-09}$	$7.22x10^{-11}$	$8.71x10^{-10}$	$6.87 x10^{-09}$	$3.57x10^{-09}$	$1.30 x10^{-10}$	$8.28x10^{-10}$
ZN-29	$4.48x10^{-09}$	$8.70x10^{-11}$	$1.81x10^{-09}$	$3.61x10^{-11}$	$7.78x10^{-10}$	$1.67 x10^{-08}$	$1.95x10^{-09}$	$2.90 x10^{-10}$	$7.38x10^{-08}$
ZN-30	$2.56x10^{-09}$	$7.00x10^{-11}$	$1.45x10^{-09}$	$3.36x10^{-10}$	$1.73x10^{-09}$	$5.88 x10^{-09}$	$5.41x10^{-09}$	$-3.10 x10^{-10}$	$2.30x10^{-09}$
ZN-31	$8.62x10^{-09}$	$9.35x10^{-11}$	$1.94x10^{-09}$	$6.55x10^{-11}$	$1.11x10^{-09}$	$7.14 x10^{-09}$	$4.99x10^{-09}$	$-5.90 x10^{-10}$	$1.83x10^{-09}$
ZN-33	$7.74x10^{-10}$	$1.02x10^{-11}$	$2.13x10^{-10}$	$1.26x10^{-10}$	$1.32x10^{-09}$	$1.66 x10^{-08}$	$3.66x10^{-09}$	$-9.80 x10^{-10}$	$1.10x10^{-08}$

ZN-34	$3.07x10^{-09}$	$6.49x10^{-11}$	$1.35x10^{-09}$	$4.44x10^{-10}$	$1.46x10^{-09}$	$3.78\ x10^{-09}$	$2.05x10^{-09}$	$-1.50\ x10^{-10}$	$1.97x10^{-09}$
ZN-35	$1.38x10^{-09}$	$3.04x10^{-11}$	$6.30x10^{-10}$	$3.32x10^{-10}$	$1.25x10^{-09}$	$9.37x10^{-09}$	$2.03x10^{-09}$	$7.84\ x10^{-10}$	$1.43x10^{-09}$
ZN-36	$7.50x10^{-10}$	$2.93x10^{-11}$	$6.08x10^{-10}$	$1.41x10^{-10}$	$1.14x10^{-09}$	$1.15\ x10^{-08}$	$2.00x10^{-09}$	$1.80\ x10^{-10}$	$3.17x10^{-09}$
ZN-38	$2.44x10^{-09}$	$8.32x10^{-11}$	$1.73x10^{-09}$	$5.10x10^{-11}$	$2.23x10^{-09}$	$8.34\ x10^{-09}$	$1.50x10^{-09}$	$-7.10\ x10^{-11}$	$9.32x10^{-08}$
ZN-40	$3.54x10^{-09}$	$1.19x10^{-10}$	$2.47x10^{-09}$	$8.89x10^{-11}$	$1.13x10^{-09}$	$1.81\ x10^{-08}$	$4.51x10^{-09}$	$-2.60\ x10^{-10}$	$3.23x10^{-09}$
Min	**$9.41x10^{-13}$**	**$1.02x10^{-11}$**	**$2.13x10^{-10}$**	**$2.01x10^{-11}$**	**$3.41x10^{-10}$**	**$3.78\ x10^{-09}$**	**<MDA**	**$-9.80\ x10^{-10}$**	**$8.28x10^{-10}$**
Max	**$1.03x10^{-08}$**	**$1.34x10^{-10}$**	**$2.67x10^{-06}$**	**$4.44x10^{-10}$**	**$1.61x10^{-06}$**	**$1.81\ x10^{-08}$**	**$5.41x10^{-09}$**	**$1.30\ x10^{-09}$**	**$9.32x10^{-08}$**
Ave.	**$3.16x10^{-09}$**	**$6.16x10^{-11}$**	**$1.40x10^{-07}$**	**$1.25x10^{-10}$**	**$7.41x10^{-08}$**	**$9.79\ x10^{-09}$**	**$2.54x10^{-09}$**	**$-1.76\ x10^{-11}$**	**$1.40x10^{-08}$**

4.3 Stable isotopes within the study area

Figure 20 shows stable isotopes ranging from -6.92‰ to -2.52‰ of $\delta^{18}O$ and -32.2‰ to -6.7‰ for $\delta^{2}H$. The stable isotopes of hydrogen and oxygen were plotted against the GMWL and the JMWL. The points ZN-11, ZN-31, and ZN-38 lie on the JLMWL, and this suggests that the boreholes were directly recharged by precipitation. The direct recharge could be facilitated by the fractured quartzites in the area. These points which lie on the JMWL are highly enriched in $\delta^{18}O$ and depleted in $\delta^{2}H$. Samples ZN-29 and ZN-40 lie below the JMWL and just above the GMWL and this suggests that there was evaporation before recharge. Spring sample ZN-27 lies above the JLMWL towards the right making it slightly depleted in both $\delta^{18}O$ and $\delta^{2}H$. The signature of the isotopic composition of the ZN-27 spring shows recycling to surface water which may have experienced evaporation before recharge. Abiye *et al*. (2015) suggest that samples that lie above the JMWL may be indicative of low humidity in the vapour as it precipitated. The spring (ZN-18) and borehole samples ZN-14, ZN-20, ZN-21, ZN-33, and ZN-35 are highly depleted in $\delta^{18}O$ and $\delta^{2}H$ and lie at the bottom left corner of the stable isotopes plot. Samples with highly depleted $\delta^{18}O$ and $\delta^{2}H$ suggest the clouds formed far from the sampling site. The Vaal dam lies directly on the GMWL suggesting that the moisture source of this dam is of a global scale because of its vast catchment. The intersection of the GMWL and the JMWL, and the range of the $\delta^{2}H$ and $\delta^{18}O$ values suggest that there is a mixing of waters meaning that the moisture is from different contributions (Leketa *et al*., 2019). It could be inferred that the precipitation of water samples lying on the GMWL could be from the coastal regions while that of the JMWL is from local dams and rivers.

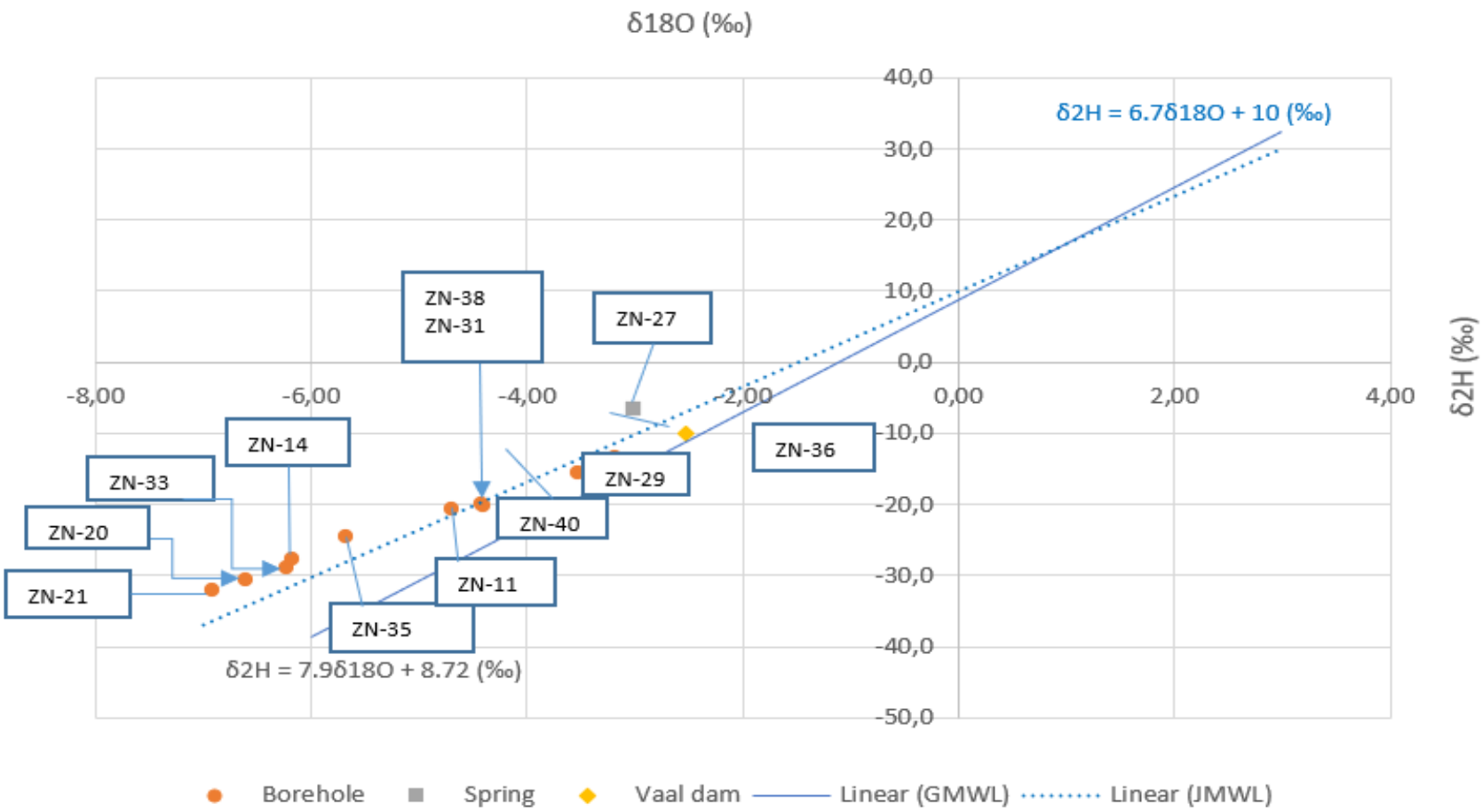

Figure 20: *A graph showing the stable isotopes in groundwater versus the Johannesburg Local Meteoric Water Line (Leketa et al., 2019) and the Global Meteoric Waterline (Terzer et al., 2013).*

The deuterium excess also referred to as the d-excess is used to measure the various ratios of δ^2H and $\delta^{18}O$ which enable scientists to determine the moisture source and decipher the atmospheric processes of the recharge rainfall (Leketa *et al*., 2019). The data in Table 3 was then used to construct the d-excess versus $\delta^{18}O$ plot in Figure 21. The d-excess values in Figure 20 range from -36.3 to -6.9‰. The d-excess of all the samples is much depleted in δ^2H and $\delta^{18}O$ suggesting that the water vapour source is from the regional circulation and the clouds travelled long distances before precipitation occurred. The d-excess results coincide with those of the stable isotopes concerning the regional circulation moisture source (Clark and Fritz, 2013). The groundwater samples have varying d-excess values, and this is indicative of various moisture sources (Aggarwal *et al*., 2012; Leketa *et al*., 2019). The variations in the d-excess values could be due to differences in the humidity and vapour during cloud formation as well as other processes such as evaporation that occur before recharge (Clark and Fritz, 2013; Abiye *et al*., 2015).

Table 3: *D-excess of groundwater samples in the West Rand.*

Sample ID	**Source**	**δ^2H (‰)**	**$\delta^{18}O$ (‰)**	**d-excess (‰)**
ZN11	Borehole	-20.8	-4.7	-21.5
ZN14	Borehole	-27.7	-6.2	-31.3
ZN20	Borehole	-30.8	-6.6	-34.3
ZN21	Borehole	-32.2	-6.9	-36.3
ZN27	Spring	-6.7	-3.0	-10.1
ZN29	Borehole	-13.5	-3.2	-11.3
ZN31	Borehole	-20.1	-4.4	-19.5
ZN33	Borehole	-29.0	-6.2	-31.7
ZN35	Borehole	-24.6	-5.7	-28.0
ZN36	Vaal dam	-10.0	-2.5	-6.9
ZN38	Borehole	-19.9	-4.4	-19.6
ZN40	Borehole	-15,7	-3.5	-13.6

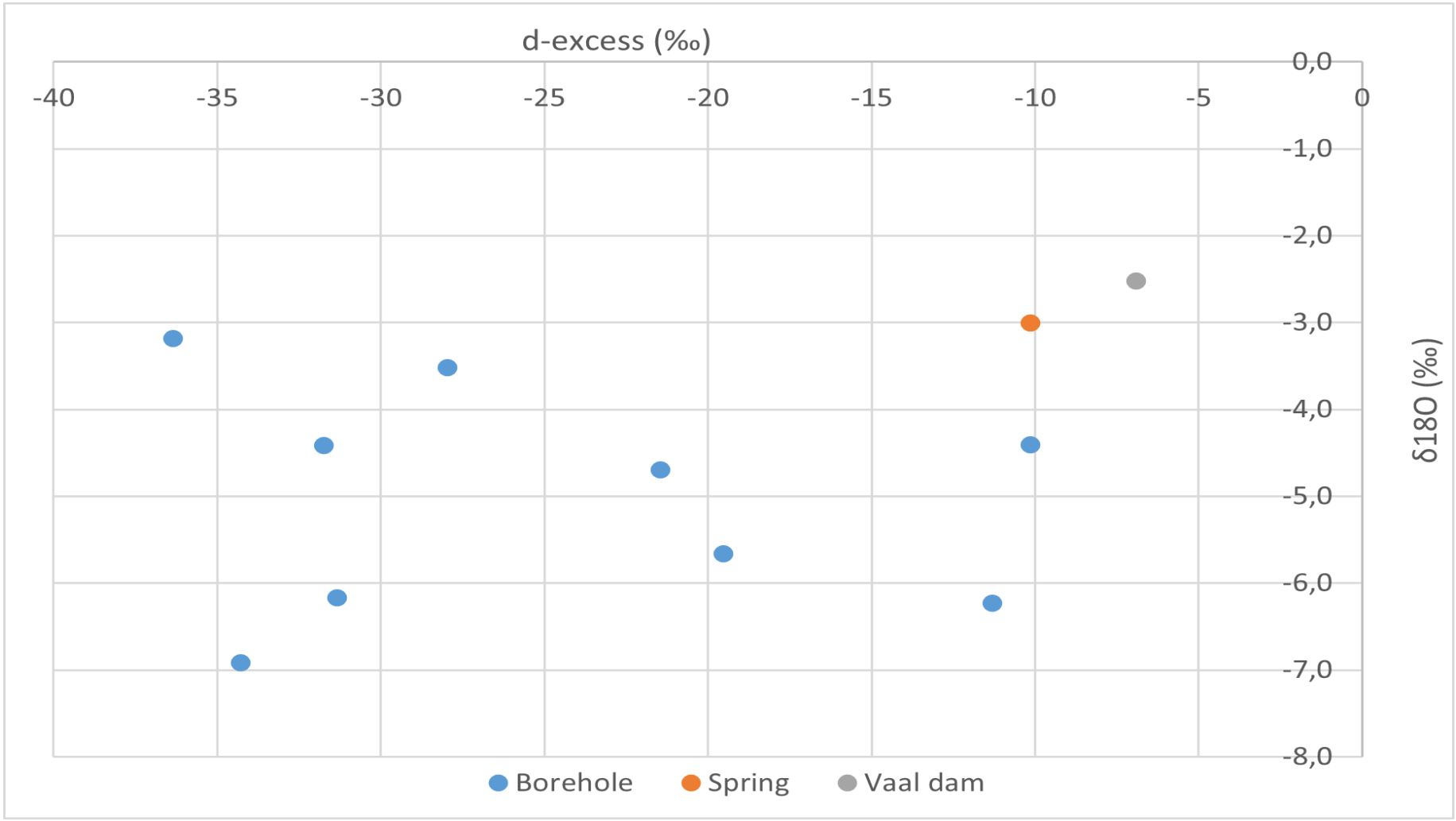

Figure 21: *The graph of d-excess against $\delta^{18}O$ for surface and groundwater samples in the West Rand.*

4.4 Tritium

Table 4 is a summation of the six tritium samples collected within the study area and Figure 23 is an illustration of the spatial distribution of these samples. Tritium is a useful tool that can be used to calculate the residence times of groundwater samples (Clark and Fritz, 2013). The half-life (12.43 years) of ^{3}H and its ability to mimic a water molecule makes it useful in determining the relative age of groundwater (Madruga *et al.*, 2009; Clark and Fritz, 2013). The range of the reported ^{3}H activities is from 9.44 mBq/L (0.8 TU) to 28.32 mBq/L (2.4 TU). The low tritium values suggest low activities and long residence times (Figure 22) which suggests long circulation times deep within the aquifer where tritiated rainfall may take long to percolate and reach the aquifer (Abiye, 2011). The activity levels of all the samples are within the acceptable WHO drinking water guideline (100 Bq/L). The spring sample ZN-27 has the highest tritium and activity concentration of 28.32 mBq/L and this suggests recent direct recharge from rainfall. The high activity concentration of this spring could be attributed to the fact that it is free-flowing and is possibly in contact with atmospheric ^{3}H.

***Table 4**: Six water samples with their activity concentration, stable isotopes, and tritium data.*

Sample ID	Description	$\delta^{18}O$ (‰)	$\delta^{2}H$ (‰)	Tritium		Activity (mBq/L)	Residence times (years)
				TU	±		
ZN-14	Borehole	-6.17	-27.73	1.8	0.3	21.24	20
ZN-27	Spring	-3.01	-6.74	2.4	0.3	28.32	15
ZN-29	Borehole	-3.18	-13.50	2.0	0.3	23.6	18
ZN-31	Borehole	-4.41	-20.14	0.8	0.2	9.44	35
ZN-35	Borehole	-5.67	-24.57	2.0	0.3	23.6	18
ZN-40	Borehole	-3.52	-15.71	1.9	0.3	22.42	19

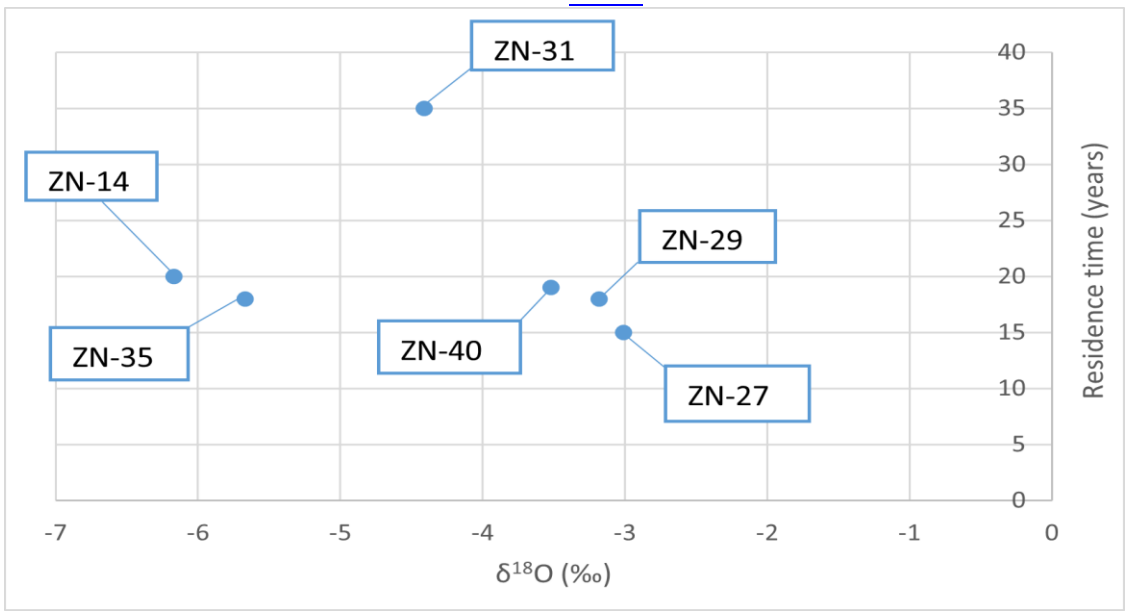

Figure 22: *A scatter plot showing the relationship between $\delta^{18}O$ and the residence time.*

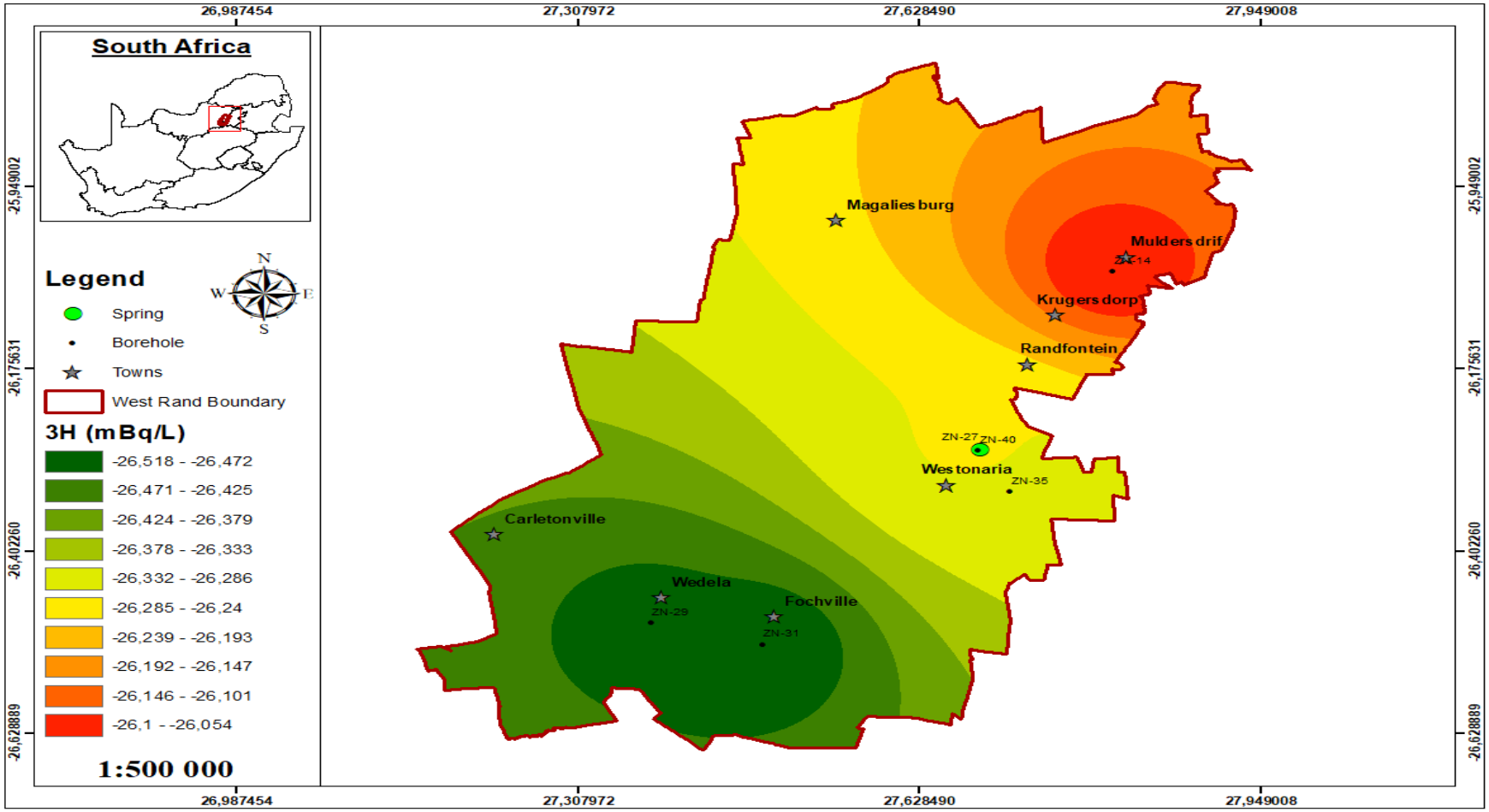

Figure 23: *A spatial distribution map for ^{3}H for six groundwater samples.*

4.5 A comparison of results from this study to previous studies

***Table 5**: Mean activity concentrations (mBq/L) for the radionuclides of interest from this study compared with the relevant drinking water guidelines and literature values.*

	^{234}U (mBq/L)	^{235}U (mBq/L)	^{238}U (mBq/L)	^{227}Th (mBq/L)	^{228}Th (mBq/L)	^{230}Th (mBq/L)	^{232}Th (mBq/L)	^{226}Ra (mBq/L)	^{210}Pb (mBq/L)	Gross-α (mBq/L)	Gross-β (mBq/L)	Reference
The West Rand, South Africa	65.34	1.31	27.2	14.25	16.72	46.6	11.03	2.30	20.35	100.19	829.0	This study
WHO	10 000	1 000	1 000	10 000	1 000	1 000	1 000	1 000	200	500	1 000	(WHO, 2011)
DWAF	-	-	890	-			228	420	-	500	1 380	(Forestry, 1996)
Gauteng, South Africa	4 710	145	3 160	202	124	690	62	360	-	6 010	6 050	(Madzivire *et al.*, 2013)
West Rand	-	-	690	-	-	-	150	-	-	-	-	(Moshupya, 2021)
Namibia	233 410			460				-	-	-	-	(Mathuthu *et al.*, 2021)
Croatia	-	7 000	101 000	-	-	-	31 800	48 300	33 500	1 048 600	811 250	(Medunić *et al.*, 2020)

Bangladesh	-	-	-	-	-	-	190	43	-	-	-	(Alam *et al.*, 1999)

Table 5 compares the results of this study with similar previous studies in different parts of the world. This study reported very low activity concentrations while other studies reported activity concentrations that were significantly greater than the allowed limits. This study reported the lowest activity concentrations compared to other similar studies within the West Rand region and this could mean that the radioactivity has reduced over time. The differences in the reported activity concentrations could be attributed to the sampling sites where samples were collected. This study collected samples from taps and boreholes in residential areas near mine tailing dumps some of which may have been properly neutralised and shielded to emit very little radiation. The study conducted by Mathuthu *et al.* (2021) reported very high uranium activity concentrations as the study was done in uranium mining regions in Namibia. The Croatian study conducted by Medunić *et al*. (2021) also yielded very high uranium activity concentrations and this could be a direct result of the unique geology of the area where coal and uranium are formed in the same setting. In the case of the Croatian study, the geology is unique, and the activity concentrations reported illustrate this. Coal is usually formed in sedimentary settings which may contain sedimentary rocks such as organic rich shale. These sedimentary rocks are often hosts of uranium (Cowart and Burnett, 1994). This study together with the conducted by Alam *et al.* (1999) in Bangladesh reported activity concentrations that were very low and well within the recommended WHO and DWAF guidelines for all the measured parameters. This suggests that the uranium and other radionuclides come in minute quantities and may thus get diluted during transport to the sampling sites.

5. Conclusion

In conclusion, the study has shown that the radiological baseline in the West Rand region is well within the recommended drinking water guidelines. Various isotopes of uranium (^{234}U, ^{235}U, ^{238}U), thorium (^{227}Th, ^{228}Th, ^{230}Th, ^{232}Th), radium (^{226}Ra), ^{3}H and ^{210}Pb have been studied with much consideration. Although these are isotopes of the same element, they are all unique and thus behave differently under different conditions. This study has reported low thorium activity concentrations, and this could be attributed to its insolubility in water. The mobility of thorium and radium is a direct consequence of the insoluble sulphate and phosphate salts they form.

The gross-α and gross-β activity concentrations are also useful tools in the identification of radionuclides present in the sample. Only one sample (ZN-30) had a gross-β activity which was above the recommended drinking water guidelines. The effective dose from ingestion was calculated to evaluate the radiological risks related to radiation exposure. The effective dose sums up all the affected organs and tissue to give the overall radiation exposure. All the samples of this study reported effective doses which are within the drinking water guidelines which state that the annual effective dose must be between 1 mSv/L and 3 mSv/yr.

The environmental isotopes and tritium data revealed evidence of multiple moisture sources from global circulation patterns. The d-excess and tritium data showed evidence of deep circulating groundwaters that had relatively long residence times. The measured physicochemical parameters revealed that the samples had an overall neutral pH. The neutral pH resulted in a moderate mean EC and this is a direct indication of the TDS in the samples. This study had lower activity concentrations as compared to other studies conducted in South Africa and other parts of the world.

The results from this study reported low activity concentrations and low effective doses from the ingestion of water over some time. Most of the samples with the highest effective dose are borehole samples suggesting that the geology, as well as the aquifer systems of the areas where the samples were collected, has an impact on the radiation levels reported. A comparison of other earlier studies showed that this study had lower activity concentrations. The results of this study may thus be used as a reference point on which policies for governing water use and radiation protection can be established.

6. Recommendations

Below is a list of recommendations to fellow researchers following the outcome of this study:

i. The samples must be analysed as soon as possible, once the radionuclides have reached circular equilibrium.
ii. The samples that reported negative activity concentrations and effective doses must be re-analysed.
iii. To assess the impact of gold mining on the water quality of the mining towns, continuous monitoring is needed.
iv. The samples could be analysed using various methods to evaluate the sensitivity of different radiation detectors.
v. More studies need to be conducted during different seasons to check if seasonal effects have an impact on the migration and dispersion of radionuclides.
vi. Further studies need to be conducted to accommodate the various exposure pathways and give a better representation of the effective dose calculated.

References

Abiye T A 2011. The provenance of groundwater in the crystalline aquifer of Johannesburg area, South Africa. *International Journal of Physical Sciences,* 6**,** 98-111.

Abiye T, Mengistu H, Masindi K and Demlie M 2015. Surface water and groundwater interaction in the upper Crocodile River Basin, Johannesburg, South Africa: Environmental isotope approach. *South African Journal of Geology,* 118**,** 109-118.

Aggarwal P K, Alduchov O A, Froehlich K O, Araguas-Araguas L J, Sturchio N C and Kurita N 2012. Stable isotopes in global precipitation: A unified interpretation based on atmospheric moisture residence time. *Geophysical Research Letters,* 39.

Akcil A and Koldas S 2006. Acid Mine Drainage (AMD): causes, treatment and case studies. *Journal of Cleaner Production,* 14**,** 1139-1145.

Alam M, Chowdhury M, Kamal M, Ghose S, Islam M and Anwaruddin M 1999. Radiological assessment of drinking water of the Chittagong region of Bangladesh. *Radiation protection dosimetry,* 82**,** 207-214.

Alexander, G V, Nusbaum, R E and Macdonald, N S 1954. Strontium and calcium in municipal water supplies. *Journal (American Water Works Association),* 46**,** 643-654.

Antunes I M H R, Neiva A, Albuquerque M, Carvalho P, Santos A and Cunha P P 2018. Potential toxic elements in stream sediments, soils and waters in an abandoned radium mine (central Portugal). *Environmental geochemistry and health,* 40**,** 521-542.

Baroni L, Cenci L, Tettamanti M and Berati M 2007. Evaluating the environmental impact of various dietary patterns combined with different food production systems. *European journal of clinical nutrition,* 61**,** 279.

Beers, R F 1945. Radioactivity and organic content of some Paleozoic shales. *AAPG Bulletin,* 29**,** 1-22.

Blowes D, Ptacek C, Jambor J and Weisener C 2003. The geochemistry of acid mine drainage. *Treatise on geochemistry,* 9**,** 612.

Boekhout F, Gérard M, Kanzari A, Michel A, Déjeant A, Galoisy L, Calas G and Descostes M 2015. Uranium migration and retention during weathering of a granitic waste rock pile. *Applied Geochemistry,* 58**,** 123-135.

Bruneton, P, Cuney, M, Dahlkamp, F and Zaluski, G. IAEA geological classification of uranium deposits. PAPERS PRESENTED, 2014. 8.

Clark I D and Fritz P 2013. *Environmental isotopes in hydrogeology,* CRC press.

Clement, C, Petoussi-Henss, N, Bolch, W, Eckerman, K, Endo, A, Hertel, N, Hunt, J, Pelliccioni, M, Schlattl, H and Zankl, M 2010. Conversion coefficients for radiological protection quantities for external radiation exposures. *International Commission on Radiological Protection, ICRP report,* 116**,** 125-137.

Cowart, J and Burnett, W 1994. The Distribution of Uranium and Thorium Decay-Series Radionuclides in the Environment—A Review. *Journal of Environmental Quality,* 23**,** 651-662.

Department of Water Affairs and Forestry, DWAF 1996. South African Water Quality Guidelines *Radioactivity.* Pretoria: Department of Water Affairs and Forestry.

Dohare D, Deshpande S and Kotiya A 2014. Analysis of groundwater quality parameters: a review. *Research Journal of Engineering Sciences ISSN,* 2278**,** 9472.

Durand, J 2012. The impact of gold mining on the Witwatersrand on the rivers and karst system of Gauteng and North West Province, South Africa. *Journal of African Earth Sciences,* 68**,** 24-43.

Durand J F 2007. Challenges associated with living in karst environments, such as the historical Cradle of Humankind.

Emsl E 1980. Method 900.0: Gross Alpha and Gross Beta Radioactivity in Drinking Water. Prescribed procedures for the measurement of radioactivity in drinking water. EPA/600/4/80/032.

European Commission 1998. On the quality of water intended for human consumption. *Official Journal of the European Communities,* 330**,** 32-54.

Faanu A, Darko E and Ephraim J 2011. Determination of natural radioactivity and hazard in soil and rock samples in a mining area in Ghana. *West African Journal of Applied Ecology,* 19.

Fuchs S, Williams-Jones A and Przybylowicz W 2016. The origin of the gold and uranium ores of the Black Reef Formation, Transvaal Supergroup, South Africa. *Ore Geology Reviews,* 72**,** 149-164.

Godel B, Barnes SJ and Maier WD 2007. Platinum-Group Elements in Sulphide Minerals, Platinum-Group Minerals, and Whole-Rocks of the Merensky Reef (Bushveld Complex, South Africa): Implications for the Formation of the Reef. *Journal of Petrology,* 48**,** 1569-1604.

Hamutoko J, Mapani B, Ellmies R, Bittner A and Kuells C 2014. A fingerprinting method for the identification of uranium sources in alluvial aquifers: An example from the Khan and Swakop Rivers, Namibia. *Physics and Chemistry of the Earth, Parts A/B/C,* 72**,** 34-42.

Hobbs P J and Cobbing J E 2007. Hydrogeological assessment of acid mine drainage impacts in the West Rand Basin, Gauteng Province.

Huang, H-H 2016. The Eh-pH diagram and its advances. *Metals,* 6**,** 23.

IAEA 2011. Exposure of the Public from Large Deposits of Mineral Residues. *IAEA-TECDOC-1660.* Vienna.

Islam R, Faysal S M, Amin M R, Juliana F M, Islam M J, Alam M J, Hossain M N and Asaduzzaman M 2017. Assessment of pH and Total Dissolved Substances (TDS) in the commercially available bottled drinking water. *Journal of Nursing and Health Sciences,* 6**,** 35-40.

Kaplan D, Seme R and Piepkho M 1995. Geochemical factors affecting radionuclide transport through near and far-fields at a low-level waste disposal site. Pacific Northwest Lab., Richland, WA (United States).

Kefeni K K, Msagati T A and Mamba B B 2017. Acid mine drainage: prevention, treatment options, and resource recovery: a review. *Journal of Cleaner Production,* 151**,** 475-493.

Kim, E and Osseo-Asare, K 2012. Aqueous stability of thorium and rare earth metals in monazite hydrometallurgy: Eh–pH diagrams for the systems Th–, Ce–, La–, Nd–(PO4)–(SO4)–H2O at 25 C. *Hydrometallurgy,* 113**,** 67-78.

Koliabina D P S, Bugai D, Avila R. 2018. Comparison of RESRAD-OFFSITE and NORMALYSA software tools for the Tessenderlo test case. *Research Gate.*

Lapworth, D J, Brauns, B, Chattopadhyay, S, Gooddy, D C, Loveless, S E, Macdonald, A M, Mckenzie, A A, Muddu, S and Nara, S N 2021. Elevated uranium in drinking water sources in basement aquifers of southern India. *Applied Geochemistry,* 133**,** 105092.

L'annunziata M F 2012. *Handbook of radioactivity analysis,* Academic Press.

Leketa K, Abiye T, Zondi S and Butler M 2019. Assessing groundwater recharge in crystalline and karstic aquifers of the Upper Crocodile River Basin, Johannesburg, South Africa. *Groundwater for Sustainable Development,* 8**,** 31-40.

Lind O, Stegnar P, Tolongutov B, Rosseland B, Strømman G, Uralbekov B, Usubalieva A, Solomatina A, Gwynn J and Lespukh E 2013. Environmental impact assessment of

radionuclide and metal contamination at the former U site at Kadji Sai, Kyrgyzstan. *Journal of environmental radioactivity,* 123**,** 37-49.

Luptáková A, Kotuličová I, Bálintová M and Demčák Š 2015. Bacterial Reduction Of Barium Sulphate By Sulphate-Reducing Bacteria. *Nova Biotechnologica et Chimica,* 14**,** 135-140.

Madruga M J, Sequeira M M and Gomes A R. Determination of tritium in waters by liquid scintillation counting. LSC 2008, International conference on advances in liquid scintillation spectrometry. Radiocarbon, 2009. Citeseer, 353-359.

Madzivire G, Maleka P, Lindsay R and Petrik L 2013. Radioactivity of mine water from a gold mine in South Africa. *WIT Transactions on Ecology and the Environment,* 178**,** 147-158.

Madzivire G, Maleka P P, Vadapalli V R, Gitari W M, Lindsay R and Petrik L F 2014. The fate of the naturally occurring radioactive materials during treatment of acid mine drainage with coal fly ash and aluminium hydroxide. *Journal of environmental management,* 133**,** 12-17.

Madzunya, D, Dudu, V, Mathuthu, M and Manjoro, M 2020. Radiological health risk assessment of drinking water and soil dust from Gauteng and North West Provinces, in South Africa. *Heliyon,* 6**,** e03392.

Magagula M. 2015. *Mapping of y-emitting radionuclides from Princess Mine Dump and the potential radiological effects on human beings.* Master of Science Mini-dissertation, North-West University.

Marshak S 2011. *Earth: Portrait of a Planet: Fourth International Student Edition,* WW Norton & Company.

Mathuthu M, Uushona V and Indongo V 2021. Radiological safety of groundwater around a uranium mine in Namibia. *Physics and Chemistry of the Earth, Parts A/B/C,* 122**,** 102915.

Mccarthy T S 2011. The impact of acid mine drainage in South Africa. *South African Journal of Science,* 107**,** 01-07.

Medunić G, Bucković D, Crnić A P, Bituh, T, Srček, V G, Radošević, K, Bajramovic, M and Zgorelec, Z 2020. Sulfur, metal (loid) s, radioactivity, and cytotoxicity in abandoned karstic Raša coal-mine discharges (the north Adriatic Sea). *Rudarsko-geološko-naftni zbornik,* 35.

Mhlongo S E and Amponsah-Dacosta F 2014. Assessment of Safety Status of Open Excavations and Water Quality of Pit Lake at Abandoned Nyala Mine in Limpopo Province of South Africa. *Sui, Sun and Wang. An Interdisciplinary Response to Mine Water Challenges, China University of Mining and Technology Press, Xuzhou***,** 395-399.

Milenkovic B, Stajic J M, Stojic N, Pucarevic M and Strbac S 2019. Evaluation of heavy metals and radionuclides in fish and seafood products. *Chemosphere,* 229**,** 324-331.

Moshupya, M P 2021. Assessment of levels of radioactivity and development of radiation protection strategy for the public in the West Rand area, South Africa.

Moshupya P, Abiye T, Mouri H, Levin M, Strauss M and Strydom R 2019. Assessment of Radon Concentration and Impact on Human Health in a Region Dominated by Abandoned Gold Mine Tailings Dams: A Case from the West Rand Region, South Africa. *Geosciences,* 9**,** 466.

Neiva A, Carvalho P, Antunes I M H R, Albuquerque M, Santos A, Cunha P and Henriques S 2019. Assessment of metal and metalloid contamination in the waters and stream sediments around the abandoned uranium mine area from Mortórios, central Portugal. *Journal of Geochemical Exploration,* 202**,** 35-48.

Nikolov J, Todorovic N, Jankovic M, Vostinar M, Bikit I and Veskovic M 2013. Different methods for tritium determination in surface water by LSC. *Applied Radiation and Isotopes,* 71**,** 51-56.

Patil P, Sawant D and Deshmukh R 2012. Physico-chemical parameters for testing of water–A review. *International journal of environmental sciences,* 3**,** 1194-1207.

Pedrobom J H, Eismann C E, Menegário A A, Galhardi J A, Luko K S, De Araujo Dourado T and Kiang C H 2017. In situ speciation of uranium in treated acid mine drainage using the diffusion gradients in thin films technique (DGT). *Chemosphere,* 169**,** 249-256.

Pintilie-Nicolov V, Georgescu P L, Iticescu C, Moraru D I and Pintilie A G 2021. The assessment of the annual effective dose due to ingestion of radionuclides from drinking water consumption: calculation methods. *Journal of Radioanalytical and Nuclear Chemistry,* 327**,** 49-58.

Protection N C O R and Measurements 1954. *Permissible Dose from External Sources of Ionizing Radiation: Recommendations of the National Committee on Radiation Protection,* US Government Printing Office.

Rachkova N and Shaposhnikova L 2020. Speciation of Radium-226 in the Components of Terrestrial and Aqueous Northern Taiga Ecosystems in a Former Radium Production Site. *Geochemistry International,* 58**,** 719-728.

Ram, R, Morrisroe, L, Etschmann, B, Vaughan, J and Brugger, J 2021. Lead (Pb) sorption and co-precipitation on natural sulfide, sulfate and oxide minerals under environmental conditions. *Minerals Engineering,* 163**,** 106801.

Robb L J, Charlesworth E G, Drennan G R, Gibson R L and Tongu E L 1997. Tectono-metamorphic setting and paragenetic sequence of Au-U mineralisation in the Archaean Witwatersrand Basin, South Africa. *Australian Journal of Earth Sciences,* 44**,** 353-371.

Rosner T 1999. The environmental impact of seepage from gold mine tailings dams near Johannesburg. *South Africa*.

Rosner T, Boer R, Reyneke R, Aucamp P and Vermaak J 2001. *A Preliminary Assessment of Pollution Contained in the Unsaturated and Saturated Zone Beneath Reclaimed Gold-mine Residue Deposits,* WRC.

Serrano-Finetti E, Aliau-Bonet C, López-Lapeña O and Pallàs-Areny R 2019. Cost-effective autonomous sensor for the long-term monitoring of water electrical conductivity of crop fields. *Computers and Electronics in Agriculture,* 165**,** 104940.

Shahid, M, Dumat, C, Aslam, M and Pinelli, E 2012. Assessment of lead speciation by organic ligands using speciation models. *Chemical Speciation & Bioavailability,* 24**,** 248-252.

Skipperud L and Salbu B 2018. Radionuclides: Sources, Speciation, Transfer and Impacts in the Aquatic and Terrestrial Environment.

Skipperud L, Strømman G, Yunusov M, Stegnar P, Uralbekov B, Tilloboev H, Zjazjev G, Heier L, Rosseland B and Salbu B 2013. Environmental impact assessment of radionuclide and metal contamination at the former U sites Taboshar and Digmai, Tajikistan. *Journal of environmental radioactivity,* 123**,** 50-62.

Tsezos M and Keller D 1983. Adsorption of radium-226 by biological origin absorbents. *Biotechnology and bioengineering,* 25**,** 201-215.

Tutu H, Cukrowska E M, Mccarthy T S, Hart R and Chimuka L 2009. Radioactive disequilibrium and geochemical modelling as evidence of uranium leaching from gold tailings dumps in the Witwatersrand Basin. *International Journal of Environmental and Analytical Chemistry,* 89**,** 687-703.

Tutu H, Mccarthy T and Cukrowska E 2008. The chemical characteristics of acid mine drainage with particular reference to sources, distribution, and remediation: The

Witwatersrand Basin, South Africa as a case study. *Applied Geochemistry,* 23**,** 3666-3684.

Unscear 2000. Sources and effects of ionizing radiation. United Nations New York.

Vercouter T, Reiller P E, Ansoborlo E, Février L, Gilbin R, Lomenech C and Philippini V 2015. A modelling exercise on the importance of ternary alkaline earth carbonate species of uranium (VI) in the inorganic speciation of natural waters. *Applied Geochemistry,* 55**,** 192-198.

Vermaak M K 2005. Review on Platinum Group Elements.

Who, World Health Organisation 2004. *Guidelines for drinking-water quality*, world health organization.

Who World Health Organization 2011. Guidelines for drinking-water quality. *WHO chronicle,* 38**,** 104-8.

Winde F 2015. Uranium pollution in South Africa: past research and future needs. *Croatian Geographical Bulletin,* 77.

Winde F, Erasmus E and Geipe G 2017. Uranium contaminated drinking water linked to leukaemia—Revisiting a case study from South Africa taking alternative exposure pathways into account. *Science of the Total Environment,* 574**,** 400-421.

Wu, Q, Xian, Y, He, Z, Zhang, Q, Wu, J, Yang, G, Zhang, X, Qi, H, Ma, J and Xiao, Y 2019. Adsorption characteristics of Pb (II) using biochar derived from spent mushroom substrate. *Scientific Reports,* 9**,** 1-11.

Yoon, Y Y, Cho, S Y, Lee, K Y, Ko, K S and Ha, K 2013. Radiochemical determination of uranium and radium isotope in natural water using liquid scintillation counter. *Journal of Radioanalytical and Nuclear Chemistry,* 296**,** 397-402.